2009

On The Nature Of The Flow In A Separated Annular Diffuser

Jason Dunn
University of Central Florida

ON THE NATURE OF THE FLOW IN A SEPARATED ANNULAR DIFFUSER

by

JASON J. DUNN

B.S.A.E. University of Central Florida, 2007

A thesis submitted in partial fulfillment of the requirements
for the degree of Masters of Science in Aerospace Engineering
in the Department of Mechanical, Materials, and Aerospace Engineering
in the College of Engineering and Computer Science
at the University of Central Florida
Orlando, Florida

Fall Term 2009

Major Professor: Jay Kapat

ABSTRACT

The combustor-diffuser system remains one of the most studied sections of the turbomachine. Most of these investigations are due to the fact that quite a bit of flow diffusion is required in this section as the high speed flow exits the compressor and must be slowed down to enter the combustor. Like any diffusion process there is the chance for the development of an unfavorable adverse pressure gradient that can lead to flow separation; a cause of drastic losses within a turbine. There are two diffusion processes in the combustor-diffuser system: The flow first exits the compressor into a pre-diffuser, or compressor discharge diffuser. This diffuser is responsible for a majority of the pressure recovery. The flow then exits the pre-diffuser by a sudden expansion into the dump diffuser. The dump diffuser comprises the majority of the losses, but is necessary to reduce the fluid velocity within acceptable limits for combustion. The topic of active flow control is gaining interest in the industry because such a technique may be able to alleviate some of the requirements of the dump diffuser. If a wider angle pre-diffuser with separation control were used the fluid velocity would be slowed more within that region without significant losses.

Experiments were performed on two annular diffusers to characterize the flow separation to create a foundation for future active flow control techniques. Both diffusers had the same fully developed inlet flow condition, however, the expansion of the two diffusers differed such that one diffuser replicated a typical compressor discharge diffuser found in a real machine while the other would create a naturally separated flow along the outer wall. Both diffusers were tested at two Reynolds numbers, $5x10^4$ and $1x10^5$, with and

without a vertical wall downstream of the exit to replicate the dump diffuser that re-directs the flow from the pre-diffuser outlet to the combustor. Static pressure measurements were obtained along the OD and ID wall of the diffusers to determine the recovered pressure throughout the diffuser. In addition to these measurements, tufts were used to visualize the flow. A turbulent CFD model was also created to compare against experimental results. In the end, the results were validated against empirical data as well as the CFD model. It was shown that the location of the vertical wall was directly related to the amount of separation as well as the separation characteristics. These findings support previous work and help guide future work for active flow control in a separated annular diffuser both computationally and experimentally.

Dedicated to you, thanks for reading.

ACKNOWLEDGMENTS

Like most others, I came to college with a “Dream Job” in mind; I wanted to be a Rocket Scientist. So I studied hard, did well, and eventually went to graduate school. I have learned more in graduate school than probably all the other years of schooling I have had, and a large amount of these lessons have taken place outside of the classroom. The most important lesson I have ever learned, more of an epiphany really, is that it is more important to have a “Dream” than to have a “Dream Job.” Through graduate school I realized this, and my dream is to help humanity colonize outerspace. When you have a dream it becomes your life goal, and your life has a purpose. My life has a purpose, and everything I do with my life is to that end, including this thesis, which I sincerely hope can become a contributing work for the sake of knowledge, science, and most importantly, humanity.

It would be rude of me not to acknowledge those who have helped and encouraged me along the way. More than anything, I have to thank my family and friends for their endless amount of support and encouragement, without them I would not be where I am today. I give my thanks to my professor, Dr. Kapat, and to all my friends at the CATER Lab, I truly feel that we are running the best lab on campus. Lastly, even though she doesn’t understand English too well, I thank my dog Cosmos for allowing me to neglect her for the past few months while I wrote my thesis.

TABLE OF CONTENTS

LIST OF FIGURES X

LIST OF TABLES XIII

NOMENCLATURE XIV

CHAPTER ONE: INTRODUCTION 1

Turbines for Power Generation 3

Background 3

Diffusion and Flow Separation 6

The Cause 7

Diffusion in Turbines and the Risk Factor in Diffuser Design 9

The Compressor Discharge Diffuser 10

Diffusers and Diffusing Flow 11

Practical Use of Diffusion in Turbomachines 15

The Compressor Discharge Diffuser 16

Active Separation Control 19

Active Separation Control Techniques 19

Flow Characterization of the Diffuser 21

The Need for Experimental Research 22

Goals for this Work 23

CHAPTER TWO: LITERATURE REVIEW 24

Diffusers in Turbines 24

Separation in Diffusers 27

The Compressor Discharge Diffuser 28
Annular Combustor-Diffuser System 29
Can-Annular Combustor-Diffuser System 30
Separation Control 32
CHAPTER THREE: METHODOLOGY 34
Annular Diffuser 34
Experimental Setup 37
Experimental Procedure 40
Testing Matrix 40
Data Collection 42
Data Reduction 43
Computational Fluid Dynamics Model 44
Flow Visualization Techniques 45
Dielectric Barrier Discharge Plasma Actuator 45
CHAPTER FOUR: FINDINGS 47
Computational Fluid Dynamics Model 47
Experimental Pressure Data 53
Separated Diffuser Data 53
Attached-Flow Diffuser Data 71
Flow Visualization 73
Plasma Actuator Discharge Performance 75
Discussion of Findings 77
CHAPTER FIVE: CONCLUSIONS 89
APPENDIX A: DOMINANCE OF TURBO-BASED POWER GENERATION 92

APPENDIX B: DRAWINGS 94

APPENDIX C: EXPERIMENTAL DATA 97

APPENDIX D: NUMERICAL PRESSURE RECOVERY CALCULATIONS 107

LIST OF REFERENCES 110

LIST OF FIGURES

Figure 1.1: Pratt and Whitney PW2037 turbofan engine (www.jet-engine.net) 4

Figure 1.2: Siemens SGT6-6000G industrial gas turbine (www.powergeneration.siemens.com)..... 5

Figure 1.3: Skateboarding analogy to diffusion [Wilson, 1984]. 8

Figure 1.4: Mollier diagram for the flow process through a diffuser 12

Figure 1.5: Can-annular combustor-diffuser system of a typical industrial gas turbine [Agrawal et al., 1998] 17

Figure 1.6: Dielectric barrier discharge plasma actuator schematic 20

Figure 2.1: Performance chart for two-dimensional diffusers [Reneau, Johnston, & Kline, 1964] 25

Figure 2.2: Annular combustor-diffuser system 29

Figure 2.3 : Can-annular combustor-diffuser system of a typical industrial gas turbine [Agrawal et al., 1998] 31

Figure 2.4: Numerical predictions demonstrate separation mitigation over an airfoil using plasma actuator 33

Figure 3.1: Diffuser cross section schematic with key dimensions 35

Figure 3.2: Diffuser 2 with static pressure ports in place 37

Figure 3.3: Experimental rig schematic 38

Figure 3.4: CAD model cross section of rig 39

Figure 3.5: Experimental rig setup with diffuser 2 in place 40

Figure 3.6: Scanivalve setup attached to static pressure ports on diffuser 2 43

Figure 3.7: DBD plasma actuator arranged on diffuser model 46

Figure 4.1: Pressure recovery along OD wall from CFD model of diffuser 2..... 48

Figure 4.2: Absolute pressure contour at Re =50,000 49

Figure 4.3: Velocity contour at Re = 50,000 49

Figure 4.4 : Absolute pressure contour at Re = 100,000 51

Figure 4.5: Velocity contour at Re = 100,000 52

Figure 4.6: Velocity vectors at Re = 100,000 showing the beginning of reverse flow 52

Figure 4.7: Pressure variation between static pressure port rows along outer wall..... 54

Figure 4.8: Pressure recovery for diffuser 2 OD, dump gap ratio equal to ∞..... 55

Figure 4.9: Pressure recovery on diffuser 2 ID, dump gap ratio equal to ∞..... 56

Figure 4.10: Pressure recovery on diffuser 2 OD, dump gap ratio equal to 1.0 58

Figure 4.11: Pressure recovery on diffuser 2 ID, dump gap ratio equal to 1.0..... 59

Figure 4.12: Pressure recovery on diffuser 2 OD, dump gap ratio equal to 0.5 60

Figure 4.13: Pressure recovery on diffuser 2 ID, dump gap ratio equal to 0.5..... 62

Figure 4.14: Circumferential pressure recovery on diffuser 2, dump gap ratio equal to ∞

..... 63

Figure 4.15: Circumferential pressure recovery on diffuser 2, dump gap ratio equal to 1.0

..... 64

Figure 4.16: Circumferential pressure recovery on diffuser 2, dump gap ratio equal to 0.5

..... 65

Figure 4.17: Pressure recovery contour on diffuser 2 OD wall, DGR = ∞ Re = 50,000

..... 67

Figure 4.18: Pressure recovery contour on diffuser 2 OD wall, DGR = ∞ Re = 100,000 67

Figure 4.19: Pressure recovery contour on diffuser 2 OD wall, DGR = 1.0 Re = 50,000 68

Figure 4.20: Pressure recovery contour on diffuser 2 OD wall, DGR = 1.0 Re = 100,000 69

Figure 4.21: Pressure recovery contour on diffuser 2 OD wall, DGR = 0.5 Re = 50,000 70

Figure 4.22: Pressure recovery contour on diffuser 2 OD wall, DGR = 0.5 Re = 100,000 71

Figure 4.23: Pressure recovery on normally attached diffuser 1 72

Figure 4.24 : Tufts on diffuser 2 with dump gap ratio of ∞..... 73

Figure 4.25: Tufts on diffuser 2 with dump gap ratio of 0.5 74

Figure 4.26: Plasma discharge on diffuser at x/L = 0.2 76

Figure 4.27: Comparison of OD wall pressure recovery on diffuser 2 with findings from Adenubi (1975) 79

Figure 4.28: Comparison between diffuser 2 pressure recovery and computational results, both at Re = 100,000 80

Figure 4.29: Schematic of flow streamlines and separation zone within the diffuser at different dump gaps 84

LIST OF TABLES

Table 3.1: Geometric features of diffuser 1 and diffuser 2 36

Table 3.2: Experimental testing matrix 41

NOMENCLATURE

A	cross-sectional area
AR	area ratio, A_2/A_1
C_p	pressure recovery coefficient
CD	compressor discharge
D	diameter
D_h	hydraulic diameter
D_g	dump gap
H	hub
h	enthalpy
ID	annular diffuser inner diameter
L	wall length
N	diffuser axial length
OD	annular diffuser outer diameter
P	static pressure
p	wetted perimeter
R	radius of axial diffuser
Re	Reynolds number

ref	reference
(R_H/R_T)	radius ratio
T	tip
ΔR	annulus height (R_T-R_H)
v	velocity at a particular point in cross section
x	distance along OD wall
η_D	diffuser efficiency
θ	diffusion angle
ρ	fluid density
o	outer
0	total condition
1	inlet condition
2	outlet condition

CHAPTER ONE: INTRODUCTION

A paradigm shift is taking place in the way the world is viewing energy production. For the first time in history the energy policy of the United States, as well as other countries, is being dictated by environmental concerns more so than financial concerns [Quirke, 2009]. Global warming and the idea that human beings are the root cause of this sudden onset of global temperature rise is creating a lot of concern for the way energy is converted and used.

Today, and for the majority of the near future, turbines will dominate the field of energy production. The Department of Energy's Annual Energy Outlook (shown in Appendix A) shows that today turbo-powered electricity generation dominates the market at over 96 percent of all means of electricity generation. In fact, the turbine market will not even drop one percent by the year 2030. The only true competitor in energy production with turbine power is solar power. However, solar power captured at the Earth's surface is limited in efficiency due to the atmosphere of the Earth. A solar power plant in Earth orbit though would be quite practical as a clean, safe, and practically endless supply of energy. Many studies have shown that space based solar power is the only viable answer to the energy demands of the world's societies. However, until the technologies advance enough for space based solar power to become a practical means of clean renewable energy generation for the world, we need to focus our efforts on improving the efficiencies and clean production of turbine produced energy.

These efforts have been under way for some time now, with advancements in turbine technologies coming out quite regularly. Improvements are usually sought in areas where

efficiencies can be raised; and this often leads to research in aerodynamic losses from current designs. The penalty from aerodynamic losses can be quite large, and even a one percent rise in turbine efficiency can be a substantial improvement in the turbine industry.

Following these principles, the current research focused on characterizing the flow in a specific portion of the turbine where aerodynamic losses are impeding technology advancements. The diffuser portion at the exit of the compressor as the flow makes its way into the combustor was studied. In this very short length of the turbine the flow is quickly decelerated from velocities of 130-170 m/s to around 40-60 m/s [Klein, 1995]. Naturally there will be huge penalties in the form of poor pressure recovery when flow is decelerated so quickly in such a short length. To compensate for these penalties the diffusion angle is kept very low so that the flow does not separate, causing an even more substantial drop in pressure recovery. However, current technology is suggesting that there may be new innovative ways to actively control the flow and keep it from separating. If this were possible then the diffusion could happen at a larger angle with no decrease in pressure recovery. This advancement would create a turbine that is more lightweight due to the decrease of axial length needed to diffuse the flow and increase the efficiency as the pressure recovery is increased. The goal of this research is thus to investigate the flow in a naturally separated diffuser and completely characterize it. Creating a better understanding of the flow behavior will then create a knowledge base for the development of active flow control in such a diffuser.

Turbines for Power Generation

The turbomachine is a fractal; no matter what level of magnification we look at it we find just as much complexities. On the large scale, the turbomachine as a whole is complex, even more so when thinking about how it becomes implemented into a power plant, producing power for entire cities. Take a closer look at a specific part of the turbomachine and you find just as much, maybe more, complexities. The geometry of the rotor blades is very precise, with small tolerances, and exotic material compositions. Take and even closer look within the rotor blade and you find a very complex arrangement of cooling channels, which had an even more complex passage getting to the blade. For such a complex machine to exist one would expect a long history of work getting to this point, and that is exactly the case for the turbomachine.

Background

There are two major uses of the gas turbine today, the aero gas turbine and the industrial gas turbine for power generation. Both operate on the exact same principles with the only major difference being that the aero-turbine is designed for a high thrust to weight ratio, meaning it is very light weight. The industrial gas turbine is not limited as much by weight, maybe only to the extent of reducing material costs.

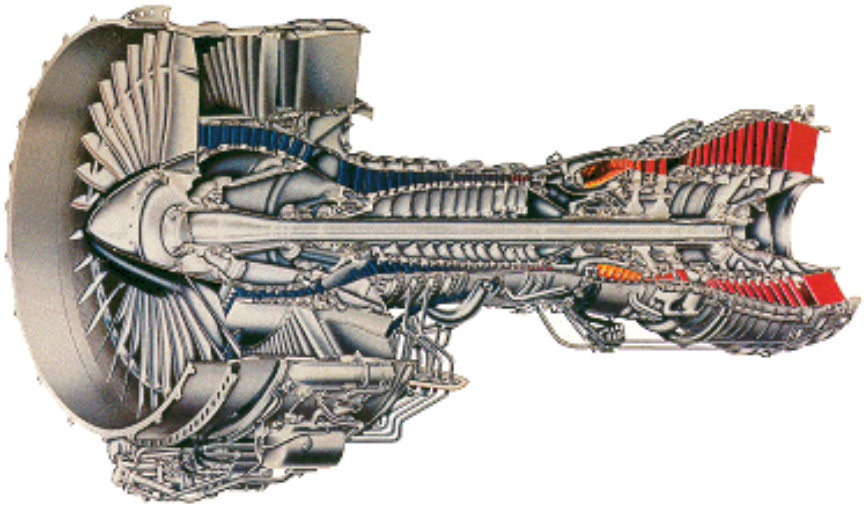

Figure 1.1: Pratt and Whitney PW2037 turbofan engine (www.jet-engine.net)

A common example of an aero gas turbine is the Pratt and Whitney PW2037 turbofan shown in Figure 1.1. The term “turbofan” refers to the fan at the inlet that drives air into the compressor and around the entire machine as by-pass air. One major difference between the turbomachine used for aero applications and that used for industrial applications is the combustor design. The majority of industrial turbines use what is known as a can type combustor system, a set of discrete combustor zones, while the aero engine will employ an annular combustor, which is seen in Figure 1.1 just after the compressor. The annular combustor works great for aero applications, but when maintenance becomes quite regular, and replacing combustor regions is needed, the can type combustor becomes more efficient.

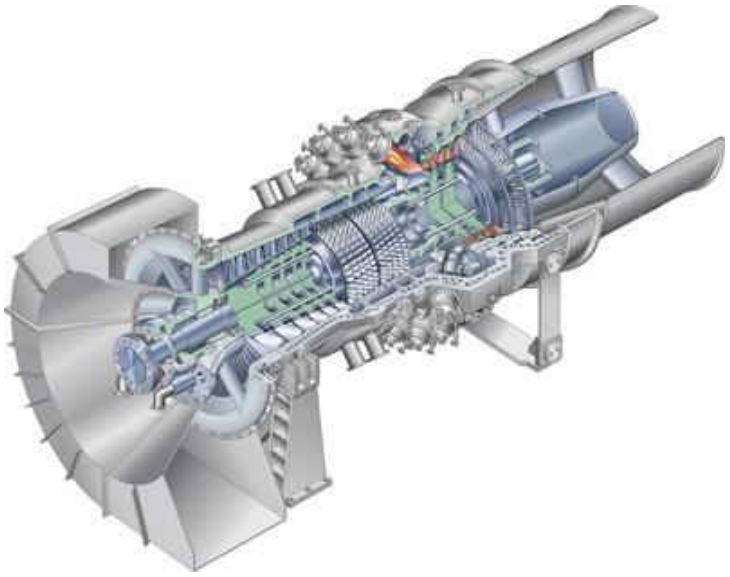

Figure 1.2: Siemens SGT6-6000G industrial gas turbine
(www.powergeneration.siemens.com)

The differences between the aero turbine and the industrial turbine can be seen by looking at the Siemens SGT6-6000G industrial gas turbine shown in Figure 1.2. These machines are orders of magnitude larger than the aero engines, and by far heavier by size. However, the mechanisms by which they both work are identical. The difference to note here though is the combustor design. The discrete can style combustors can be seen in Figure 1.2. Later on it will become evident what the differences are between the annular combustor and the can style combustor. Both of which have a complicated upstream geometry to slow the flow velocity coming out of the compressor to reasonable speeds for combustion.

Much of the historical development of the turbomachine has been in the creation of an efficient compressor. The turbine, with flow going from high to low pressure will usually work with high efficiency, however the compressor is quite the opposite and up until the

beginning of the twentieth century compressors operated at isentropic efficiencies lower than 50 percent [Wilson, 1984]. As a result of low efficiency, axial compressors were abandoned for multistage centrifugal compressors with their higher efficiencies. It was not until 1926 that any further research was performed on axial compressors when A.A. Griffith outlined his theory on airfoil theory and compressor design. Today it is now widely known that although a fluid can be rapidly accelerated through a passage and sustains a small or moderate loss in total pressure, the same cannot be said for a rapid deceleration of fluid. This is because large losses result due to severe stall caused by a large adverse pressure gradient. Therefore, to limit the total pressure losses during flow diffusion it is necessary for the rate of deceleration in the blade passages to be severely restricted. It is for this reason that axial compressors have many stages [Dixon, 2005]. Interestingly, in 1899 Charles Parsons created an eighty-one stage compressor, an all time record, capable of attaining 70 percent efficiency. Today researchers are still looking for ways to create more efficient diffusion processes in the turbomachine.

Diffusion and Flow Separation

In its most simplistic form, diffusion is the conversion of dynamic head into stream pressure, dominating the design criteria of all turbomachinery. The majority of aerodynamic and hydrodynamic losses in turbomachines are the result of an area of local or general boundary layer separation as a result of a local or general level of diffusion too large for the boundary layer to overcome. This principle, and the lack of understanding thereof was the contributing factor to the late arrival of efficient pumps and compressors

until a good number of years into the 1900's, and more so the delay of a practical gas-turbine engine until the mid 1930's [Wilson, 1984].

The Cause

Diffusion can occur on isolated surfaces and within ducts, where for the desired reduction in flow velocity to occur the boundary layer must remain attached. At any point that separation occurs the main flow will form a jet that dissipates into turbulence, causing significant losses. In this regard, flows with laminar boundary layers at the inlet, or with thick turbulent boundary layers will not be capable of withstanding as much diffusion without separation as will thin turbulent boundary layers [Wilson, 1984]. Some work has been done using thin turbulent boundary layers to allow a larger amount of diffusion.

To visualize the concept of diffusion lets use the analogy of a group of skateboarders racing along a walled track approaching a hill as shown in Figure 1.3. Consider that the skateboarder in the center of the track has enough velocity to make it over the hill, but the skater along the outside is brushing against the wall, which is reducing his/her velocity so much that there is an insufficient amount of kinetic energy to make it over the hill. If the skater along the wall comes to rest half way up the hill and begins rolling back the skaters next in line to him/her will have to leave the wall in an analogy of separation.

Figure 1.3: Skateboarding analogy to diffusion [Wilson, 1984].

If the skateboarders along the wall are to make it over the hill the skaters next in line, travelling at higher speeds, must give them a hand to *drag* them up the hill. In the case of laminar boundary layers the viscous *drag* forces are relatively small, which is why laminar flows will experience separation with a reasonably small amount of diffusion. For the case of turbulent flows, there is an energy exchange by way of the working fluid in the inner region of the boundary layer from the regions of higher energy. In the skateboarding analogy, the skateboarders with higher velocities, farther from the wall, would exchange places with the slower skateboarders closer to the wall. By switching positions like this the skateboarders would ensure that no skateboarders could go very slow in conditions of excessive diffusion, or slope. Now of course, there will be some

energy losses during this exchange of positions, but these losses are minuscule when compared to the losses if separation was allowed to occur [Wilson, 1984].

From this explanation of diffusion it is then clear that the term *separation* is the incident when the main flow is undergoing a pressure rise, or rate of diffusion, large enough to bring the boundary layer to rest. In most cases a vortex forms just downstream of the separation point. Within this vortex the flow will often reverse direction against the wall. This vortex however creates another boundary surface to the flow and in some cases is influential enough to modify the pressure distribution to the point that the flow will *reattach* to the wall downstream, creating a *separation bubble*. In these instances the overall flow losses are rather small, even though a significant region of the flow may exist in the separation bubble. Although in most cases, the flow will not reattach, but rather remain separated as a high velocity jet flow away from the wall. The jet tends to dissipate in turbulent mixing and at this point the pressure recovery ceases to increase [Wilson, 1984].

Diffusion in Turbines and the Risk Factor in Diffuser Design

It is clear that diffusion plays a very significant role in the design and function of a turbomachine, however there tends to be design issues between upstream and downstream parts of the turbine, where one region may be experiencing separation. The issues occur because separation is typically thought of as a steady-flow phenomenon, but on the contrary, it is often quite unsteady. In some cases an unsteady flow separation that travels up and down a wall without ever producing a jet-like separation may produce maximum diffusion, but can be detrimental to a downstream blade row that was designed

to accept a fully attached flow. Component designers are usually caught up in this problem, blaming poor performance of one component on the velocity profile provided by an upstream component [Wilson, 1984].

It is now understandable that increasing the diffusion of kinetic energy to pressure energy can make significant gains in efficiency and specific power in a turbomachine. One must be cautious though not to become too greedy with the degree of diffusion in the design. One method for designing a diffuser for maximum diffusion may be to start with a small diffusion angle, or area ratio, and then slowly increase it to find the location where separation will occur. Unfortunately though, the area ratio that causes separation will likely allow the separation to move back upstream to area ratios that were previously small enough not to separate, in the end letting the entire flow field become separated.

To explain this idea we can imagine, for instance, that one of the skateboarders from earlier decides that he/she wants to sell his/her skateboard after losing the race by placing a single advertisement in the classifieds of the Sunday paper. The skateboarder may know that the skateboard is worth anywhere from $50 to $100, and would be sure that it would sell for $40 then. He/she could make more money though by asking $50, $70, or even $100, but the chances of it not selling will continually increase. If the advertisement asks $150 for the skateboard it will surely not sell. The excess of greed has lost the sale.

The Compressor Discharge Diffuser

The compressor discharge diffuser, also known as the *pre-diffuser* for its role of slowing the flow while maximizing pressure recovery before entering the *dump diffuser* portion just before the combustor, serves a very important role in any turbomachine. But, before

the compressor discharge diffuser is explained in detail it is necessary to review the concept of diffusion and the purpose a diffuser can have in fluid mechanics.

Diffusers and Diffusing Flow

A diffuser is a device that is designed to reduce the velocity of a fluid flow as well as increase the fluid static pressure. Geometrically, the diffuser is quite simple. In turbomachines, where the flows are generally subsonic, the diffuser is simply a channel that has an increasing cross sectional area in the flow direction [Dixon, 2005]. However simple, the diffuser's basic characteristics are still not completely understood; much to the avail of a long history of investigation by many researchers. Diffusers are useful in many internal flow applications where the flow needs to be slowed down with minimal losses [Sovran & Klomp, 1967]. The alternative to the diffuser is a *sudden expansion* that creates large pressure losses by decelerating the flow very abruptly.

The process of diffusion can be visualized on a Mollier diagram, Figure 1.4, by following the change of state between point 1 and 2. The change in pressure from p_1 to p_2 is dependent on the change in velocity from v_1 to v_2.

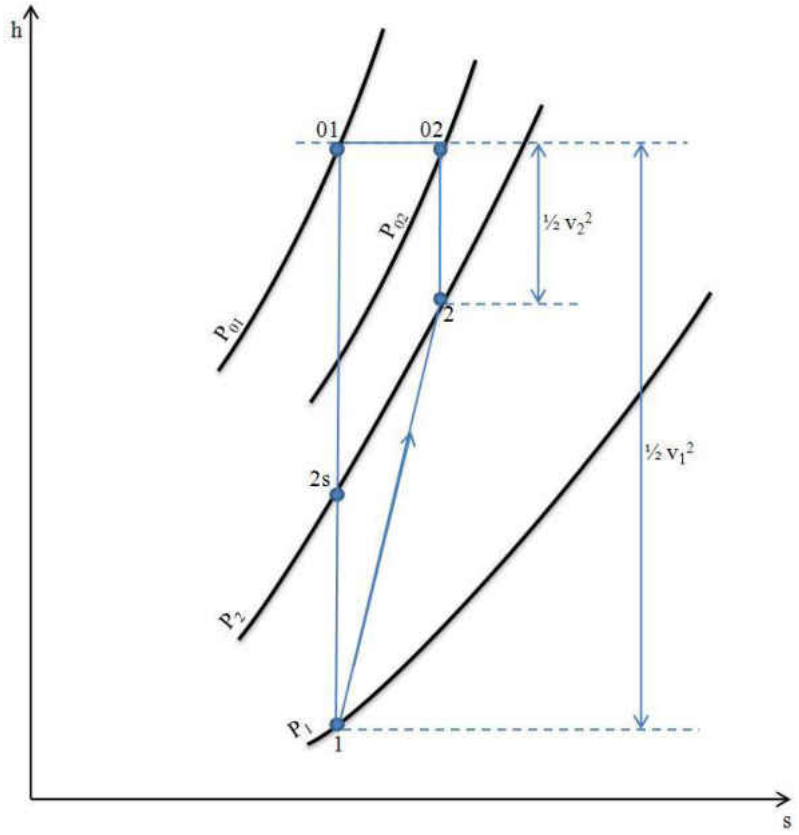

Figure 1.4: Mollier diagram for the flow process through a diffuser

In any diffuser design it is important to understand the performance that such a design will have. There are a couple ways to express the actual performance of the diffuser. It can be expressed as the ratio of actual enthalpy change to isentropic enthalpy change as seen on the Mollier diagram in Figure 1.4, or as the ratio of the actual pressure recovery coefficient to an ideal pressure recovery coefficient [Dixon, 2005].

Assuming that for a steady and adiabatic flow in a stationary passage the total enthalpy remains the same between states, $h_{01} = h_{02}$, we can say that:

$$h_2 - h_1 = \frac{1}{2}(v_1^2 - v_2^2)$$ Equation 1

Identically, for the isentropic process from point 1 to point 2 the change in enthalpy becomes:

$$h_{2s} - h_1 = \frac{1}{2}(v_1^2 - v_{2s}^2)$$ Equation 2

The *diffuser efficiency*, otherwise known as the *diffuser effectiveness*, η_D, can be defined as the ratio between the isentropic enthalpy rise to the actual enthalpy rise through the diffuser.

$$\eta_D = \frac{h_{2s} - h_1}{h_2 - h_1}$$ Equation 3

By considering that for incompressible flows the density will remain constant, the isentropic enthalpy rise can be represented as:

$$h_{2s} - h_1 = \frac{p_2 - p_1}{\rho}$$ Equation 4

Substituting Equation 1 and Equation 4 into Equation 3 the diffuser efficiency becomes:

$$\eta_D = \frac{2(p_2 - p_1)}{\rho(v_1^2 - v_2^2)}$$ Equation 5

It is most practical to be able to express the diffuser effectiveness in terms of pressure only, and this can be accomplished by writing the difference between actual and isentropic enthalpies for the p_2 pressure line on the Mollier diagram as:

$$h_2 - h_{2s} = (h_2 - h_1) - (h_{2s} - h_1)$$ Equation 6

Finally, substituting Equation 6 into Equation 3 with a bit of manipulation gives:

$$\eta_D = \frac{1}{1 + (p_{01} - p_{02})/(p_2 - p_1)}$$ Equation 7

Now, it is often needed to express the diffuser effectiveness as a ratio of an actual pressure recovery coefficient to an ideal pressure recovery coefficient. The pressure recovery coefficient can be defined as the ratio of the actual pressure rise of a diffuser to the maximum attainable pressure rise at a given flow rate considering one-dimensional flow; or in other words, the dynamic pressure [Sovran & Klomp, 1967].

$$C_p = \frac{P_2 - P_1}{\frac{1}{2}\rho v^2}$$ Equation 8

For an incompressible flow the first law of thermodynamics can be expressed as:

$$\frac{p_1}{\rho} + \frac{1}{2}v_1^2 = \frac{p_2}{\rho} + \frac{1}{2}v_2^2 + \frac{\Delta p_0}{\rho}$$ Equation 9

where Δp_0 signifies the loss in total pressure, $p_{01} - p_{02}$. We can then use the continuity equation to show that:

$$\frac{v_1}{v_2} = \frac{A_2}{A_1} = AR$$ Equation 10

A quick manipulation of Equation 9 and Equation 10 shows that the ideal pressure recovery is only a function of the area ration, AR:

$$C_{pi} = 1 - \frac{1}{AR^2}$$ Equation 11

Finally, using Equation 11, we can rewrite Equation 9 as:

$$C_p = C_{pi} - \frac{\Delta P_0}{\frac{1}{2}\rho v_1^2}$$

which means that the diffuser efficiency is simply:

$$\eta_D = \frac{C_p}{C_{pi}} \qquad \text{Equation 12}$$

By examining Equation 12, when the diffuser efficiency is at a maximum the total pressure loss is at a minimum for a given static pressure rise. It can be shown [Dixon, 2005] quite simply that the maximum pressure recovery does not coincide with the maximum diffuser efficiency. In fact, as the diffuser angle is increased beyond the divergence that yields the maximum diffuser efficiency, the actual pressure rise will continue to grow until the losses in the total pressure can equilibrate with the theoretical increase in the pressure recovery that was produced by the increase in the diffuser angle.

Practical Use of Diffusion in Turbomachines

Diffusion plays a key role in many parts of the typical turbomachine. Between rotor and stator blades in the compressor, the flow will diffuse since the blades produce an overall reduction in relative velocity of the working fluid. The extent of energy that can be transferred to the fluid is dictated by the degree at which the velocity can be reduced in the rotor. This concept leads designs focused on maximum reduction as to minimize the number of stages required for a preferred work output [Sovran & Klomp, 1967].

In some cases a diffuser portion can be found between two turbines in a *free turbine arrangement*. In this case, the diffuser is necessary to reduce the flow velocity to a level

that is efficient for the operating conditions of the downstream turbine. Also, a diffuser may be used downstream of the turbine where an increase in pressure rise is beneficial. Just like the condenser in the steam turbine, this diffuser will help reduce the back pressure in the turbine, effectively increasing the expansion ratio and the allowable work output [Sovran & Klomp, 1967].

Another important use of the diffuser is found in the region between the exit of the compressor and the inlet to the combustor. The diffuser is used in this regard to reduce the fluid velocity enough so that it cannot blow out the flame within the combustion chamber. The typical arrangement in an annular machine is to have a *pre-diffuser* at the exit of the compressor that slows the flow velocity while maintaining a sufficient amount of pressure recovery followed by a *dump diffuser*, a large region that is fairly inefficient in pressure recovery, but necessary to reach the low fluid velocity needed before entering the combustor [Sovran & Klomp, 1967].

The Compressor Discharge Diffuser

The compressor discharge diffuser (CD diffuser), also known as the *pre-diffuser*, is the area of interest for this investigation. Providing a very important role in creating desirable flow conditions in the combustor, the CD diffuser is an area of much investigation and research. If the effectiveness of this diffuser can be increased the need for the highly inefficient dump diffuser that follows can be reduced, or perhaps become less important in flow stabilization.

Purpose

Typical gas turbine engines employ a diffuser system between the compressor discharge and the combustor(s) inlet comprising of the CD diffuser and a dump diffuser as shown in Figure 1.5. The general purpose of this diffuser system is to decelerate the compressor discharge flow and to distribute the air evenly around various holes on the combustor liner. This process, of course, must be accomplished with a low total pressure loss, as losses have an adverse impact on thermal efficiency. More so, the flow regime that the diffusers create must be uniform around the combustor liner to achieve a stable and efficient combustion [Agrawal et al., 1998].

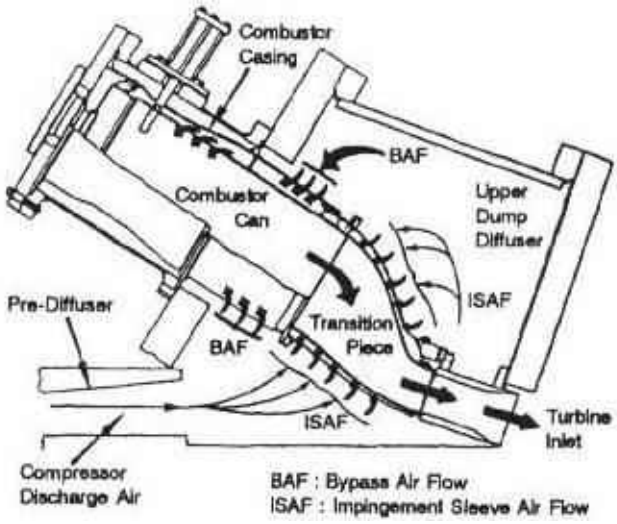

Figure 1.5: Can-annular combustor-diffuser system of a typical industrial gas turbine [Agrawal et al., 1998]

The CD diffuser plays an especially important role in pressure recovery, where nearly all the recovered pressure through the diffuser system comes from the CD diffuser, and the majority of the losses come from the dump diffuser. However, the CD diffuser is not capable of fully reducing the flow velocity to the low speeds needed at the combustor.

This gives special importance to the dump diffuser in current applications. At the CD diffuser exit a sudden expansion occurs as the flow enters the dump diffuser. A recirculation zone will be created at the sudden expansion, which although helps to maintain a stable flow condition regardless of the engine operating conditions, will create large pressure losses [Agrawal et al., 1998].

Drawbacks and Limitations of Current CD Diffuser Technology

While the CD diffuser may currently be the best design option for creating the appropriate flow conditions between the compressor and the combustor, there are still some major limitations on its capabilities. Specifically, the large dependence on the dump diffuser to create the final reduction in flow velocity is detrimental on efficiency. The limitation on CD diffuser length, and the corresponding limitation on diffusion angle, results in a less than acceptable flow velocity reduction. Even though appreciable performance can be achieved with large diffusion angle annular diffusers, (since the hub surface is present to guide the flow radially outward) this diffusion angle is still not sufficient to slow the flow enough to make the dump diffuser only needed for distributing the flow into the combustor [Sovran & Klomp, 1967].

If there were a way to use a CD diffuser with a greater diffusion angle without sacrificing pressure recovery, the need for the dump diffuser to reduce the flow velocity would be greatly reduced. This in turn would put less stringent requirements on the size and design of the dump diffuser, which currently produces so much of the losses in this compressor-combustor diffuser system. If the CD diffuser could slow the flow relative to the desired flow velocities needed at combustor inlet then the dump diffuser would only be needed to re-distribute the flow appropriately around the combustor lining. This fact is widely

recognized and much research has gone into finding possible ways to control the flow in the CD diffuser. The most practical way that the CD diffuser could slow the flow to lower velocities is if the diffusion angle was increased, however this would result in larger pressure losses due to the increased adverse pressure gradient and the large possibility of separated flow. Therefore, in conjunction with a wider angle CD diffuser, some type of active flow control will be needed to keep the flow from separating in the diffuser.

Active Separation Control

Active separation control is simply any technique that has the ability to control the flow regime in such a manner as to create more acceptable flow conditions. In the case of the CD diffuser an active separation control mechanism could be used in conjunction with a large angle of diffusion to prohibit separation. This in turn would allow for a smaller more efficient diffuser design. The techniques for active separation control can vary from geometric design characteristics within the diffuser to mechanisms that are capable of keeping the flow attached.

Active Separation Control Techniques

A very simple separation control technique is found in the typical aircraft engine. The compressor delivers air at a velocity around 200 m/s to a coaxial diffuser, which has been designed to efficiently reduce the velocity to fewer than 100 m/s. However, the flow entering the combustor just downstream needs to be at a much lower velocity. A simple solution has been to place a break in the smooth wall of the diffuser to accurately locate

the diffusion to yield maximum diffusion [Wilson, 1984]. This technique, although controlled, still invites the flow to separate, which should always be avoided.

This brings up the idea of an active separation control mechanism that is capable of keeping a normally separated flow completely attached throughout the diffuser. One technique that holds much promise and is even in use today is the dielectric barrier discharge. This flow control technique has been used successfully for lift augmentation and separation control on lifting surfaces ranging from fixed wings to wind turbines; from flow separation and tip casing clearance flow control to reduce losses in turbines to controlling flow surge and stall in compressors [Corke et al., 2009].

Dielectric Barrier Discharge Actuator

In the past decade the interest in dielectric barrier discharge (DBD) actuators has increased quite substantially. The reason being the several desirable features DBD actuators possess. DBD actuators are fully electronic with no moving parts; they have a very fast time response, and have a very low mass making them quite useful in turbine applications, especially in aircraft turbines where cost cutting is always necessary. Also, DBD actuators are very efficient in conversion of power to fluid momentum [Corke et al., 2009].

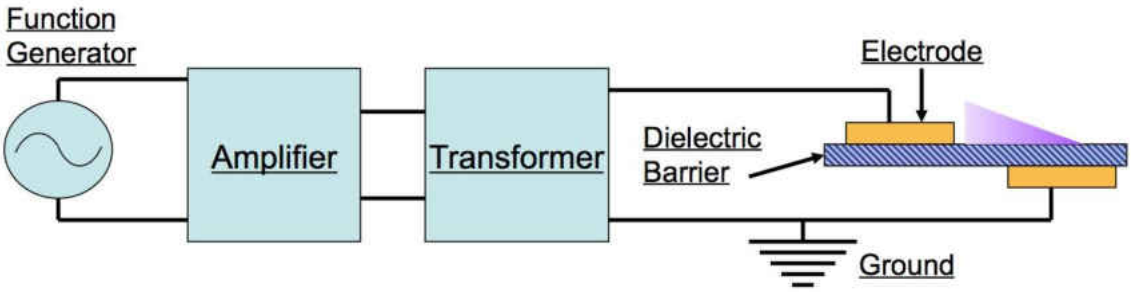

Figure 1.6: Dielectric barrier discharge plasma actuator schematic

A typical DBD actuator is depicted in Figure 1.6. This schematic is of a typical laboratory DBD actuator, but works on the same principle as one used in industry applications. A dielectric barrier, a material with low conductivity and high dielectric constant, such as acrylic is sandwiched between two electrodes. The dielectric barrier surface is the flow surface, and the electrode on the flow side is small enough to not disrupt the flow, on the order of a fraction of a millimeter. A function generator supplies an AC signal to an amplifier, which increases the signal on the order of kilo hertz sending it through a transformer to bump up the voltage to the order of five to fifteen kilo volts. The supply of this high voltage signal causes the air on the fluid side of the dielectric barrier just above the covered electrode to ionize. The ionized air is generally called *plasma* and is blue in appearance when observed in a dark space. This plasma, in the presence of the electric field create by the electrode configuration, creates a body force vector that acts on the ambient air. This body force is the mechanism by which aerodynamic flow control can be accomplished [Corke et al., 2009].

Flow Characterization of the Diffuser

Although DBD actuators hold a lot of promise for active flow control techniques in turbine applications, there is still much research needed for it to become practical. The mechanism by which momentum coupling between the plasma and the fluid flow is still not completely understood, especially on geometries more complicated than the typical flat plate flow used in laboratory experiments [Jayaraman et al., 2008]. For this reason, more research is needed to characterize the flow in a naturally separated annular diffuser before attempts to control the separation can be made. Both computational and

experimental research is needed in this discipline, however; first and foremost, a strong experimental regime needs to be established as a basis for future studies.

The Need for Experimental Research

There are two essential reasons that a complete understanding from an experimental standpoint had to be made: First, this research has focused on a three-dimensional annular diffuser. The majority of previous research focused primarily on the study of either a two dimensional diffuser or at most a three-dimensional rectilinear diffuser. Neither case lends complete authenticity to the real case scenario of a real turbine application where the diffusion happens along an annulus. Secondly, as advanced as computational fluid dynamics (CFD) has become, it still is not accurate enough to simulate conditions containing high adverse pressure gradients. In such flow regimes experimental data has been found to be highly important to verify CFD predictions [Cherry et al., 2008]. Even with simple cases, such as a two-dimensional airfoil with trailing edge separation, a variation in results was found when compared to several large-eddy simulation models. Furthermore, no one model was in close agreement with the experimental data [Mellon et al., 2003].

Previous works [Cherry et al., 2008] stressed the need for a rigorous database of experiments on separated flow to compare with CFD calculations. This must be accomplished before significant advances in separated flow predictions can exist. Furthermore, experimentalists are still studying, for the most part, two-dimensional models merely because of the savings in computational and experimental time. However, two-dimensional flows are often affected by three dimensionalities [Cherry et al., 2008].

Goals for this Work

Clearly, the need for experimental research on separated flows in an annular diffuser is very much needed. Such work could lead the way to the development of methods that would control the separation, improving turbine efficiency in an area that researchers have been struggling to find improvements for some time now. The goals of this thesis are to answer two rather simple questions regarding the flow in a naturally separated annular diffuser. First, how does the flow behave in such a diffuser: Is it predictable? Is it comparable to CFD calculations? Secondly, can this understanding create enough of a foundation to accurately design methods to control the flow separation? From the previous investigations there is some assurance that a hypothesis can be made that supports these goals; that yes, a study of the flow experimentally can create a foundation for future work in active flow control.

CHAPTER TWO: LITERATURE REVIEW

In spite of a rather large amount of investigation, the diffuser still remains one of the least understood parts of the turbine. Although geometrically simple, the diffuser portions found in a turbine are always plagued with the majority of the losses found in the turbine. In the early days of the turbomachine the turbine was far more advanced than the compressor, in some cases the compressor was just a turbine in reverse, causing huge losses obviously. In fact, for many decades' turbomachines needed an external power input because the compressor efficiency was too low to produce positive work [Wilson, 1984]. This chapter will look at the work that has been performed to develop the diffuser portions of the turbine to the technology of the present. Special interest, of course, will be paid to the CD diffuser and the characterization of separation in such an annular diffuser. Investigations on controlling this separation will also be looked into.

Diffusers in Turbines

Any literature on the annular combustor-diffuser system, including the CD diffuser, is largely based off investigations on diffusers, both two-dimensional and three-dimensional. Early investigations on diffusers were usually studied on a two dimensional model. This was quite limiting in terms of comparison to actual diffusers in turbomachines that of course are three-dimensional. Now, while the investigation of a two dimensional diffuser saves both computational time and experimental time, two-dimensional flows are often affected by three dimensionality [Cherry et al., 2008]. For instance, Obi et al. (1993) utilized an end wall separation control system to force the flow

in the experiment to remain two-dimensional; perhaps compromising any comparisons to mathematical models.

There exists a few works that stand as the basis for most other works on diffusers. The work done by Reneau, Johnston, and Kline (1964) on two-dimensional diffusers has become a standard reference when choosing performance characteristics for a diffuser. Testing was performed with air as the working fluid, covering a wide range of inlet turbulent boundary layer thicknesses. The most common representation of these results, shown in Figure 2.1, is a contour plot of pressure recovery as a function of area ratio, AR, and a non-dimensional length, N/W_1.

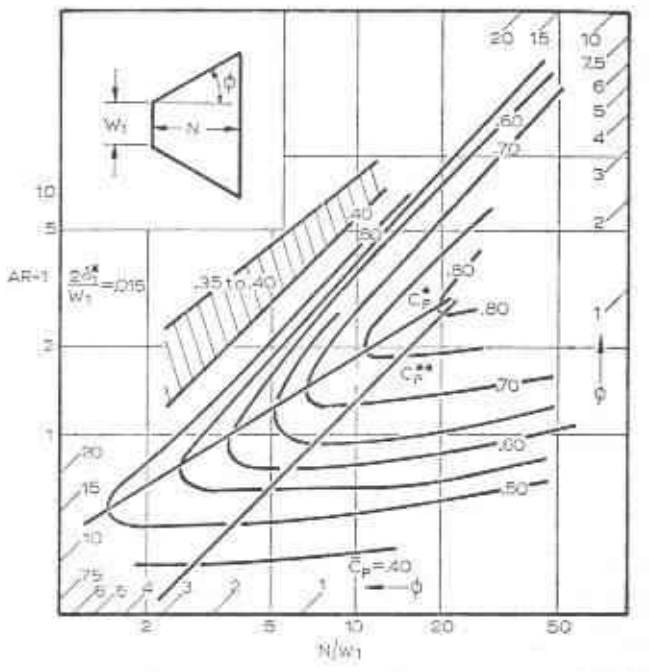

Figure 2.1: Performance chart for two-dimensional diffusers [Reneau, Johnston, & Kline, 1964]

Probably the most important aspect of the work done by Reneau et al. was the way in which the data was represented. By using a logarithmic scale to express the data, lines of

constant Φ (θ in terms of this papers nomenclature) appear as a series of parallel lines. Sovran and Klomp (1967) note the importance of this plot for the majority of work done by their group at Stanford. Conveniently, the geometry of a particular diffuser can be drawn from a particular value of Φ on the chart [Sovran and Klomp, 1967].

Following the work by Reneau et al., Sovran and Klomp in 1967 produced a very extensive work on several three-dimensional diffuser configurations that has become the foundation of nearly all current studies on diffuser technology today. Over one hundred wood diffuser geometries were tested in a test facility with free discharge conditions. The application of a free discharge condition allowed for easy access to the diffuser for flow visualization studies and for replacing the diffusers after each test. The experiments were conducted with incompressible inlet flows ($M<0.3$) at a Reynolds number between 4.8×10^5 and 8.5×10^5 and a single inlet velocity profile thanks to swirl vanes upstream of the diffuser [Sovran and Klomp, 1967].

A very significant part of the work by Sovran and Klomp (1967) was a comparison of typical results to a list of industry turbines. It was found that optimum diffuser geometries occur at an area ratio that is independent of the combination of diffusion angles and radius ratios employed. The radius ratio range studied was between 0.55 and 0.70, and showed a pretty well matching when compared this with typical numbers from industry used turbomachines. Furthermore, it was found that velocity profile at the discharge of the diffuser is largely dependent on the inlet velocity profile and the amount of distortion produced within the diffuser [Sovran and Klomp, 1967].This is quite important for the

case of the CD diffuser, where exit flow conditions are very important in terms of design of the dump and combustor inlet conditions.

Separation in Diffusers

The majority of diffuser data comes from two-dimensional tests, and those tests on three-dimensional diffusers typically do not attempt to address the flow separation phenomena. But there is a problem with relying on two-dimensional flow separation data for a three-dimensional diffuser. Also, in many cases where separation is studied it is often induced and controlled by some sort of separation control system. Obi et al. (1993) used a very high aspect ratio coupled with an intricate endwall separation system just to force the flow to be two-dimensional. Later tests by Kaltenbach et al. (1999) used a Large Eddy Simulation (LES) model to simulate the results by Obi et al. (1993) finding that the data did not satisfy two-dimensional mass conservation. The mean velocity profiles on the centerline indicated a 15% gain in mass flow rate at the area where the flow reattached downstream of the separation bubble [Cherry et al., 2008].

One of the most recent investigations studying a three-dimensional diffuser with separation was performed by Cherry et al. (2008). The goal was to compile test data of three-dimensional diffusers that could be used to compare against CFD predictions, in hopes of creating a more robust CFD model for such an unpredictable flow regime. Using water as the working fluid, two diffuser models were tested. Each had a rectangular cross section in which the sides and top walls each had a divergence to them. Magnetic resonance velocimetry (MRV), a technique similar to a medical magnetic resonance imaging (MRI) was used to visualize the flow and collect velocity data at various cross

sections. These tests showed that the separation was initiated near the sharp corner of the wall. Furthermore, the separation bubble never became two-dimensional, but rather developed unevenly down the expanding side of the diffuser. The flow reattached downstream of the diffuser outlet. The two diffusers differed very little geometrically, but the findings showed that these small variations drastically affected the magnitude and location of the separation [Cherry et al., 2008]. To further validate the MRV velocity data Cherry et al. provided static pressure measurements along the wall. The pressure recovery was seen to rise rapidly throughout the beginning of the diffuser until around x/L = 0.7, where the reverse flow spread across the top wall. The pressure recovery in the reverse flow region remained linear; validating that the flow was indeed separated [Cherry et al., 2009].

The Compressor Discharge Diffuser

The compressor discharge diffuser makes up the first part of the combustor-diffuser system; a widely researched section of the turbine. Many studies have investigated the aerodynamic performance of this system mostly to better understand how to create optimum flow conditions entering the combustor. These investigations are usually split between those studying industrial gas turbines and those studying turbines for aircraft operations or the like. The primary difference is usually the industrial gas turbine has a can style combustor arrangement whereas aircraft turbines have an annular combustor arrangement. In both cases though, the CD diffuser is essentially identical, with the biggest difference being the diffusion angle.

Annular Combustor-Diffuser System

Much of the research in the annular combustor-diffuser system, Figure 2.2, is involved with the spacing of the front of the flame tube within the dump diffuser portion. It is of interest to understand how this distance between the exit of the CD diffuser and the front of the flame tube affects the performance within the upstream CD diffuser. The common non-dimensional testing variable is the dump gap ratio, which is defined as the ratio of the distance between the exit of the CD diffuser and the front of the flame tube by diameter of the CD diffuser exit, shown in Equation 13.

$$DGR = \frac{D_G}{\Delta R} \qquad \text{Equation 13}$$

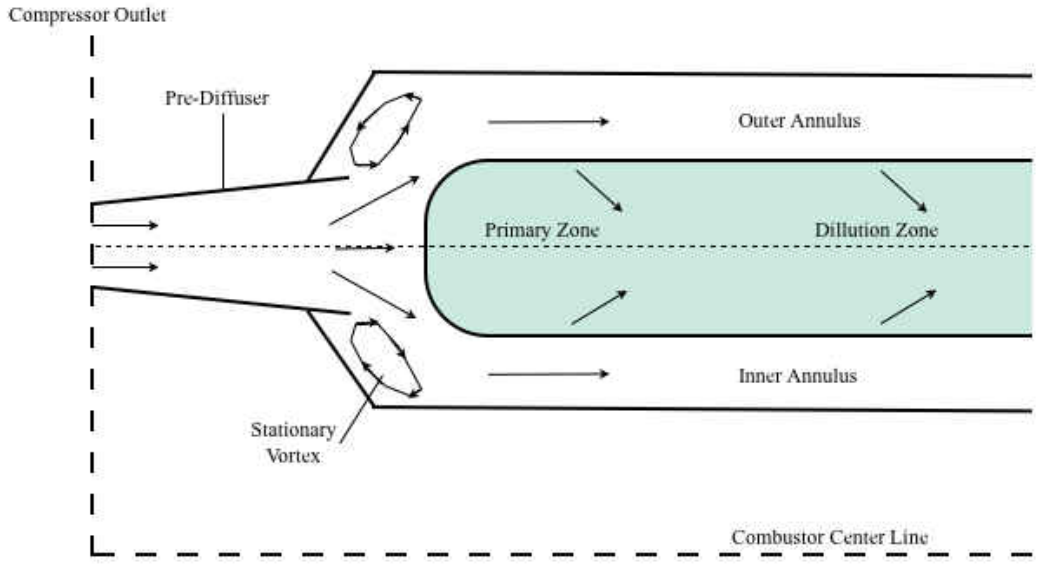

Figure 2.2: Annular combustor-diffuser system

Work by Fishenden and Stevens (1977) begin investigations on the dump gap ratio after the advent of the high bypass ratio engine. The high bypass ratio engine was capable of

achieving a high pressure ratio across the compressor with a relatively small gas generator flow. This led to very small annulus heights within the CD diffuser, guiding a stricter tolerance in manufacturing and the chance for flow distortion due to geometry flaws. Fishenden and Stevens studied the trade off's between a small dump gap, which allows the CD diffuser to reach maximum pressure recovery, to larger dump gaps that restrict pressure recovery growth, but allow for a further decrease in flow velocity needed for combustion. Surprisingly, it was found that decreasing the dump gap size beyond a certain extent, while allowing for better pressure recovery within the CD diffuser, would in fact decrease overall performance of the system. The total losses in the combustor-diffuser system at small dump gaps are on the order of 80% decreasing to less than 65% for larger dump gaps. These findings suggest that a large portion of losses occur downstream of the CD diffuser [Fishenden & Stevens, 1977]. Srinivasan et al. (1990) backed up the earlier work by Fishenden and Stevens showing that while maximum pressure recovery within the CD diffuser occurs around a dump gap ratio of about 0.7, the overall maximum pressure recovery through the entire combustor-diffuser system occurs at dump gap ratio around 1.0 [Srinivasan et al., 1990].

Can-Annular Combustor-Diffuser System

As seen in Figure 2.3, the combustor-diffuser system for a can-annular style system is rather different than the annular combustor-diffuser system. The most obvious difference is that with the can-annular system there is distinct combustor regions comprised of several "cans" situated annularly. Nevertheless, the CD diffuser portion remains essentially the same geometrically, with the only main difference being that for the can-

annular system the diffusion angle is not as large as for the annular system. The dump region for the can-annular arrangement is much different though, where the upper dump region is supplied by air moving between the two cans, taking a more arduous path than the upper dump region on the annular arrangement.

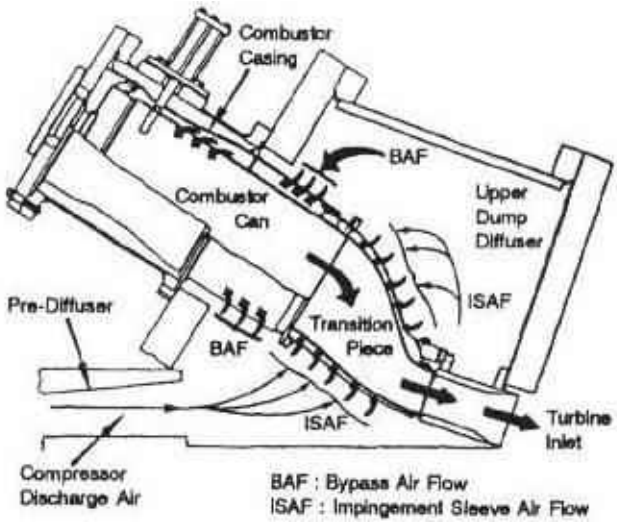

Figure 2.3 : Can-annular combustor-diffuser system of a typical industrial gas turbine [Agrawal et al., 1998]

Work by Agrawal et al. (1998) investigated the airflow in the can-annular combustor-diffuser system both experimentally and computationally. This study remains today as a very important basis for future studies, as the experimental rig was a full 360-degree three-dimensional annular rig one-third the scale of a real machine. Due to the complexity of the geometry, the amount of measurement data was fairly restricted. However, it was found that at the exit of the CD diffuser the static pressure was not uniform, disproving the long lasted assumption of a uniform exit condition into the dump. More so, it was found that a dynamic pressure head of approximately 1.2 at the inlet to the CD diffuser was lost throughout the system, primarily throughout the dump diffuser

portion. While these findings helped advance computational models in ways that no other studies had yet done, the experimental setup prohibited the amount of data that could be collected within the CD diffuser. Although it was found that the exit conditions of the CD diffuser were not uniform, it was not shown what exactly was happening within the CD diffuser to create such flow non-uniformities [Agrawal et al., 1998].

Separation Control

All the work discussed so far has addressed a plaguing problem in the turbine world: the relentless losses found within the diffuser. We are now prepared, more than ever, to find realistic solutions to this problem. Many solutions have been tried, all with the geometric arrangement of the CD diffuser and the dump diffuser proportions, but nothing yet has been too promising, just acceptable. Maybe the only promising way to completely overcome these losses is to use an active separation control technique to allow for greater diffusion with minimal losses in the CD diffuser, the portion of the combustor-diffuser system responsible for the majority of the pressure recovery as found by countless studies.

Numerical studies have been reinforced with experimental data showing the effectiveness of dielectric barrier discharge plasma actuators in controlling the flow separation. Corke et al. (2009) studied the reattachment of turbulent boundary layer separation across the suction side of an airfoil. The results, very similar to what is depicted in Figure 2.4, showed that the plasma discharge was quite effective in decreasing the magnitude of the separation. The study found that the pressure recovery was increased with the use of the

plasma discharge and the separation bubble reattached much earlier than without the use of plasma [Corke et al., 2009].

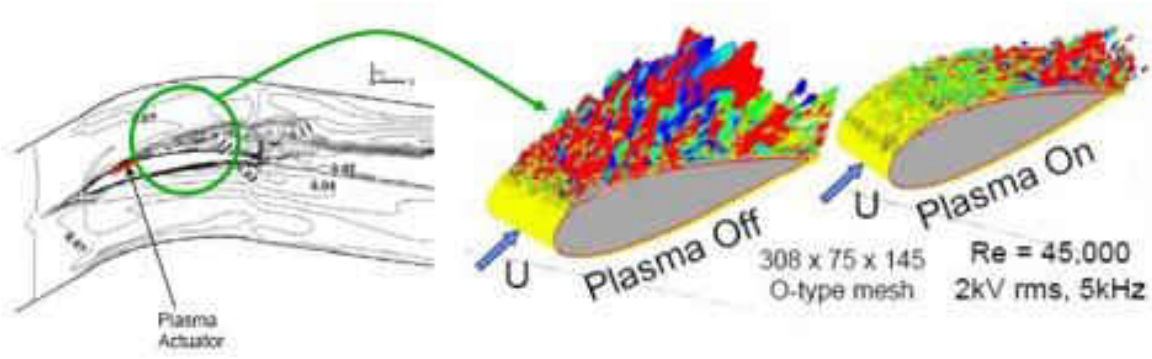

Figure 2.4: Numerical predictions demonstrate separation mitigation over an airfoil using plasma actuator

A recent study by Singh and Roy (2008) worked to find the impact of electrode spacing along with a variation in applied voltage, and how this compared with numerical solutions. It was found that the magnitude of the induced velocity from the plasma discharge increased with an increase in the amplitude of the operating rf potential; however the velocity was not affected by the change in the frequency of the rf potential. Likhanskii et al. (2008) also note that an increase in the applied voltage amplitude increases the duration of the active phase, which in turn allows the plasma to propagate further downstream. It was also discovered that the majority of the acceleration from the induced flow was located above the actuator, and not too much downstream. This work has shown that plasma actuators have the ability to promote boundary layer attachment on airfoils at a high angle of attack, or more simplistically; diffusers [Singh & Roy, 2008].

CHAPTER THREE: METHODOLOGY

The essential plan for this investigation was to study two different three-dimensional annular diffuser models: one with naturally separated flow and one with naturally attached flow. The diffuser with separated flow was studied to gain a better understanding on the separated flow characteristics so that active flow control methods could be developed. The diffuser with normally attached flow served as the control, a replication of a typical CD diffuser in industry use. The diffusers were tested for different Reynolds numbers and with different dump gap ratios. Additionally, a computational fluid dynamics model was designed to compare results against. Also, some experiments were done in the application of a dielectric barrier discharge plasma actuator to help show what would be needed for future studies incorporating an active flow control mechanism.

Annular Diffuser

Following previous work [Sovran & Klomp, 1967] two straight walled annular diffusers were designed. Figure 3.1 shows a cross sectional schematic of the diffuser. Typically four parameters are needed to quantify the geometry of such a diffuser: the diffusion angle of the inner and outer walls, the inlet radius ratio, and a non-dimensional length. For this investigation the diffusion angle for the inner wall is zero, thus diminishing some complexity in fabrication and testing. The average wall length was chosen as the characterizing length based on the fact that the most important pressure gradient is that which is dependent on the wall length [Sovran & Klomp, 1967].

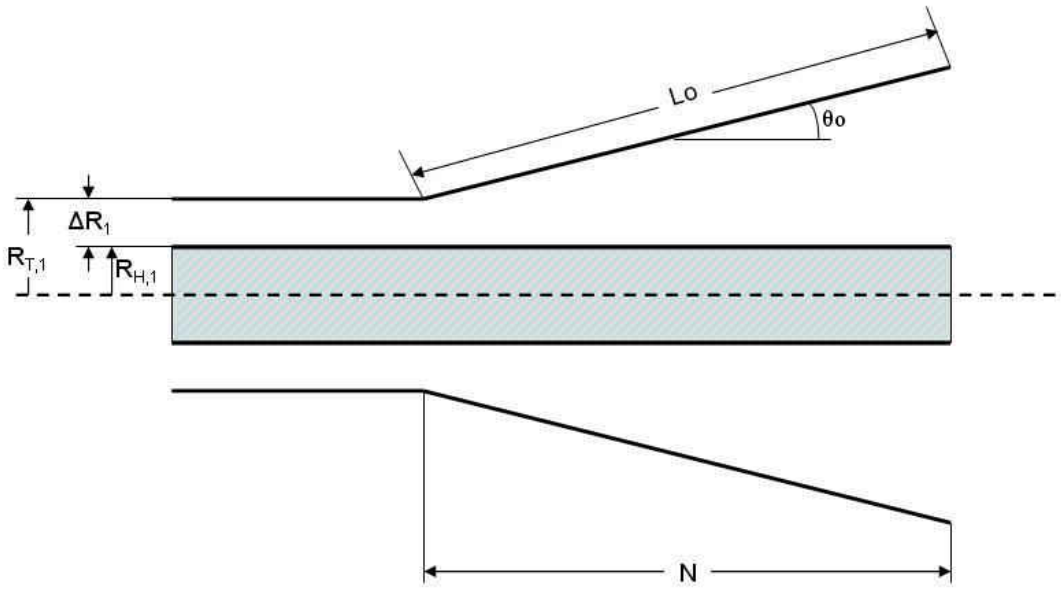

Figure 3.1: Diffuser cross section schematic with key dimensions

Two diffusers were fabricated and tested. The first diffuser, Diffuser 1, was made to replicate the General Electric 8362 turbine CD diffuser as outline by Sovran and Klomp (1967). Diffuser 2 was based off the geometries of Diffuser 1, however the diffusion angle of the outer wall was increased to 15 degrees to ensure a separated flow. Table 3.1 details the key dimensions of both diffuser prototypes.

Table 3.1: Geometric features of diffuser 1 and diffuser 2

Dimension	Diffuser 1	Diffuser 2
Diffusion angle, θ_o	9 deg	15 deg
R_{H1}	2.108 cm	2.108 cm
R_{T1}	3.896 cm	3.896 cm
ΔR_1	1.788 cm	1.788 cm
A_1	33.73 cm^2	33.73 cm^2
A_2	88.35 cm^2	138.18 cm^2
AR	2.6	4.1
L_o	11.572 cm	11.834 cm
N	11.4 cm	11.4 cm

The diffusers were made by Stereo-Lithography method, SLA, from Mydea Technologies in Orlando, Fl. The thickness of the diffuser wall was $1/8^{th}$ of an inch. Building the diffusers of SLA was done for two important purposes: First, the components where the plasma is applied must all be non-conductive so as not to interfere with the plasma. Although this investigation does not attempt to apply plasma, foresight allows for ongoing tests well into the future. Secondly, the diffuser model is clear allowing for flow visualization and non-intrusive measurement techniques such as Particle Image Velocimetry (PIV), Schlieren photography, and smoke wire visualization.

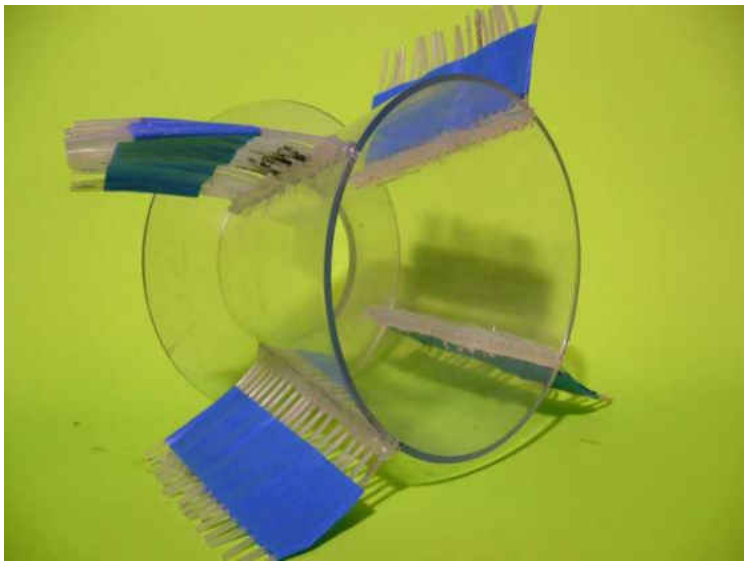

Figure 3.2: Diffuser 2 with static pressure ports in place

Figure 3.2 shows Diffuser 2 with the static pressure taps in place. There are a total of four rows of taps spaced 90 degrees from each other along the outer wall. Each row has a total of 20 pressure taps 2.54 mm apart, totaling 80 taps in all. The pressure taps where 15 mm in diameter drilled normal to the wall surface. Additional circumferential taps were placed along regions where the separation was occurring. These taps were placed on diffuser 2 on one segment of the diffuser between two rows of the streamwise pressure taps. Four taps were placed at three different circumferential locations at x/L = 0.2, 0.4, and 0.6, totally twelve circumferential pressure taps.

Experimental Setup

An open loop wind tunnel was built such that the diffusers could be attached at the exit of the tunnel. Figure 3.3 shows a schematic of the experimental rig. The flow was supplied by a Spenser 645 CFM Vortex Blower. Downstream of the blower the flow traveled through a Preso 2 inch low loss venturi flow meter. Following the venturi was a plenum

that helped diminish any instability in the flow coming from the blower. A three inch diameter pipe came out of the plenum, made a 90 degree turn and proceeded towards the diffuser. About 14 hydraulic diameters upstream of the diffuser inlet the flow turned from a pipe flow to an annular flow. This distance upstream was sufficient enough to ensure the flow was fully developed by the time it reached the diffuser inlet. While the experimental rig was designed for a uniform flow at the diffuser inlet it must be stated that the likely hood of this happening in practice, both in this experiment, and in industry applications is quite unlikely. Any uniform flow can easily be tripped by any minuscule imperfection in the rig. Let it be noted that the velocity profile at the diffuser inlet might easily be subject to swirl or flow tripping.

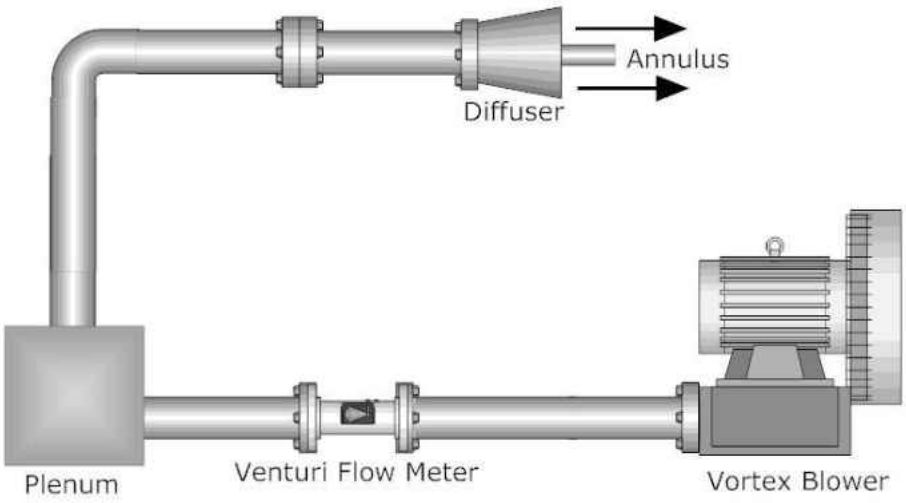

Figure 3.3: Experimental rig schematic

Figure 3.4 shows how the flow was diverted from strictly pipe flow to an annular flow. An inner pipe was mounted at two locations: at the center of the outer pipe 14 hydraulic

diameters from the diffuser inlet and then downstream of the diffuser exit. This ensured that the flow surfaces before, through, and after the diffuser remained undisturbed.

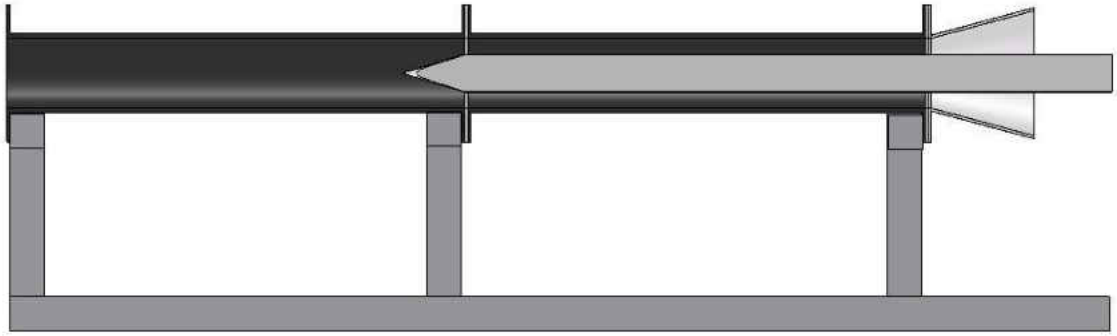

Figure 3.4: CAD model cross section of rig

The experimental rig design was ideal as it allowed for diffuser prototypes to be easily swapped out for rapid testing. Figure 3.5 shows an image of the experimental rig assembled with Diffuser 2 in place. A vertical wall was set in place for the experiments that tested the separation effect when a rough simulation of the "dump diffuser" was in place downstream of the CD diffuser. This wall was made of ¼ inch acrylic and was adjustable for dump gap ratios of 0.5, 1.0, and ∞ (no wall at all). The dump gap ratios chosen in this study represent values used in the work by Fishenden and Stevens (1967) and by Srinivasan et al. (1990). These values are quite realistic to turbine operating conditions.

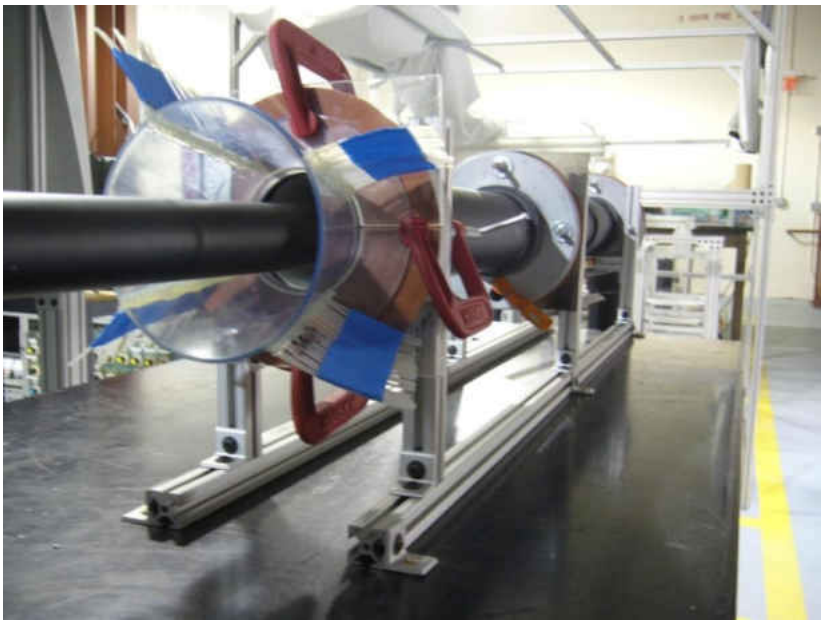

Figure 3.5: Experimental rig setup with diffuser 2 in place

Experimental Procedure

Testing Matrix

A wide range of tests were conducted on the two diffuser models. The primary scope of the tests was to study the flow characteristics at different Reynolds numbers and dump gap ratios. So, eight tests were conducted, six on diffuser 2 and two on diffuser 1. Table 3.2 covers the testing matrix.

Table 3.2: Experimental testing matrix

Test #	Diffuser	Reynolds #	DGR
1	2	5×10^4	0.5
2	2	5×10^4	1.0
3	2	5×10^4	∞
4	2	1×10^5	0.5
5	2	1×10^5	1.0
6	2	1×10^5	∞
7	1	5×10^4	∞
8	1	1×10^5	∞

The Reynolds numbers are based off the inlet hydraulic diameter, where the hydraulic diameter for an annulus can be defined as:

$$D_h = \frac{4A}{p} \qquad \text{Equation 14}$$

It is simple to derive the hydraulic diameter for an annulus:

$$D_h = \frac{4(\pi R_{T1}^2 - \pi R_{H1}^2)}{2\pi R_{T1} + 2\pi R_{H1}}$$

Simplifying,

$$D_h = \frac{2(R_{T1} + R_{H1})(R_{T1} - R_{H1})}{R_{T1} + R_{H1}}$$

Since D = 2R, the hydraulic diameter for the annulus is simply:

$$D_h = D_{T1} - D_{H1} \qquad \text{Equation 15}$$

Although these Reynolds numbers are not nearly on the order of actual turbine operation conditions they do hold some significance. The work done by Cherry et al. (2008)

investigated separated flow in a three-dimensional diffuser at low Reynolds numbers up to 3 x 10^4, and the work by Sovran and Klomp (1967) while not investigating the separation phenomena did however study flow through a three-dimensional diffuser at operation conditions at Reynolds number of 6 x 10^5. In addition to this, Sovran studied an annular design while Cherry did not. So in some regard the current study may help tie the two previous aforementioned works together.

The works by Cherry et al. (2008) and Sovran and Klomp (1967) were used merely as a basis for designing the current experiment. The current experimental rig was limited to run at Reynolds numbers no higher than 1 x 10^5, making it impossible to match Sovran and Klomp (1967) testing conditions due to structural issues with the rig. The testing conditions of Cherry et al. (2008) were much too low to come close to replicating a real machine, so the current testing conditions were chosen to lie between the two previous works.

Data Collection

A Scanivalve system was used to measure the static pressure readings from the pressure taps along the outer wall, Figure 3.6. Sixty measurements were taken at each port with a frequency of 100 Hz. The flow was regulated via a gate valve just downstream of the vortex blower exit. The valve was adjusted while using an Omega HHP-805 Pressure Meter to monitor the venture meter until the correct flow rate was reached. A pressure tap was also placed on the outer wall just upstream of the diffuser inlet. This pressure, P_i, was used as the reference pressure.

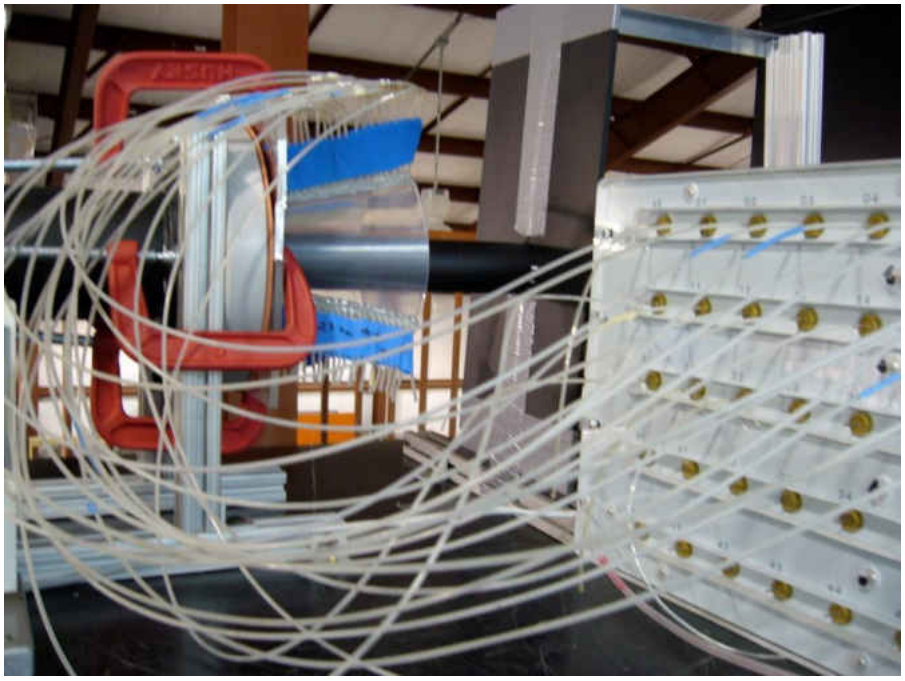

Figure 3.6: Scanivalve setup attached to static pressure ports on diffuser 2

The Scanivalve system was compared against an Airflow Developments LTD Type-4 Manometer to guarantee accuracy.

Data Reduction

The dimensionless pressure recovery coefficient was compared against the dimensionless distance along the outer wall, which was normalized by the wall length. The wall length was chosen as the normalizing factor since the most pertinent pressure gradient is that which is dependent on the outer wall length. For the current investigation all reference conditions are taken at the diffuser inlet. The reference pressure was the absolute pressure taken from a static pressure port at the inlet on the outer annulus. The reference velocity was deduced from the inlet geometry and the pre-set flow rate.

The raw pressure data collected was imported into Excel for data processing, where the uncertainty in the data was estimated using the Kline and McClintock (1953) method. There were four rows of pressure measurements along the diffuser so that any variation along the annulus of the outer wall could be found. After comparing the individual rows to one another it was clear whether or not the variations were very large. This would determine whether or not an average of the four rows was needed to ensure sound results.

Computational Fluid Dynamics Model

For comparison purposes, a CFD analysis was run using Fluent on a two-dimensional diffuser having the same geometries and inlet conditions as Diffuser 2. A Standard K Omega Model was used with a defined inlet velocity matching the Reynolds numbers from experimental testing and a pressure outlet matching the average barometric pressure measured during experimental runs. The density was assumed constant because the Mach number at the inlet of the diffuser was less than 0.3, the typical transition point to a compressible flow regime. Using the same convention for calculating pressure recovery with the experimental results, the pressure recovery is presented from the CFD model predictions for both Reynolds numbers. In addition to pressure recovery plots of pressure and velocity contours are presented to help visualize the predictions of the CFD model.

It was known that the CFD results would not compare well to the experimental data for reasons discussed previously. Therefore, the CFD results were generated purely as rough initial proof that Diffuser 2 would have separated flow. It was understood that this model was highly inaccurate; however, the point was not to understand the separation but merely to show that it would exist.

Flow Visualization Techniques

Having sound experimental results is often accomplished by using some sort of flow visualization technique to confirm the measured findings. For this investigation two flow visualization techniques were used; smoke and tufts. The smoke visualization was supplied by a standard fog machine, injecting the fog into the wind tunnel before the conversion from pipe flow to flow around the annulus. The tufts were applied at x/L of 0.2 intervals along the OD wall, using sewing thread. For both visualization methods a Panasonic 3CCD camcorder was used to capture both video and still images of the flow. Post processing of the smoke visualization made it unclear of the flow characteristics, so images of these findings are left out, however, the post processing of the tufts is very clear, and is presented in the findings. The post processing of the tuft images involved adjusting the contrast and balance to make the tufts stand out among the rest of the diffuser materials.

Dielectric Barrier Discharge Plasma Actuator

Some preliminary investigations using plasma were also carried out. These tests were merely to become familiar with the DBD plasma actuator; no real goals were set for controlling the flow. Figure 3.7 shows the plasma actuator configured on the diffuser model. The electrodes used were copper tape with conductive adhesive. The thickness of the tape was on the order of a fraction of a millimeter, so the impact it could have on the flow was negligible. Notice that the flow side electrode width is smaller than the insulated electrode width. Also, standard electrical tape was used to insulate the electrode.

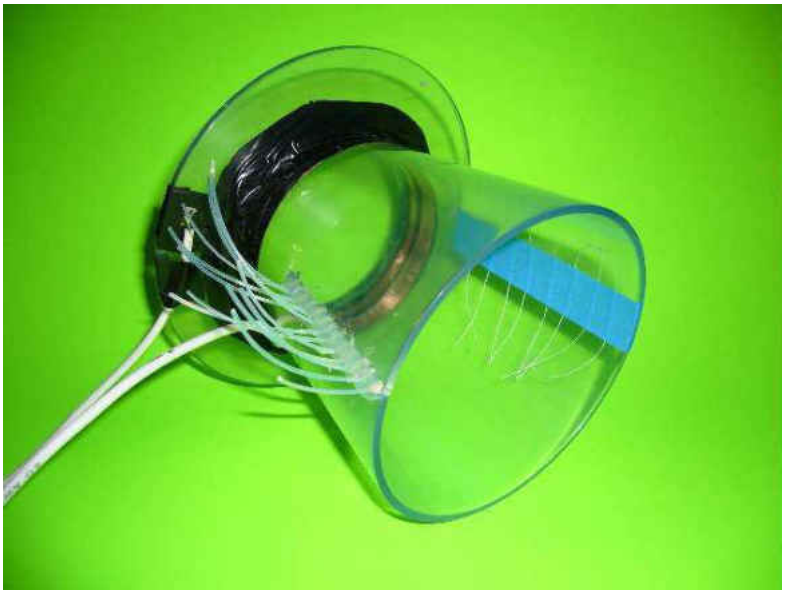

Figure 3.7: DBD plasma actuator arranged on diffuser model

Unlike the typical setup for a DBD plasma actuator, as previously discussed, there were a few shortcomings with the setup used that may have not allowed for the full potential that the plasma may have provided. Primarily, an amplifier was not used to increase the frequency of the signal to the range of kHz. In fact, the set up was quite simple: a 15 kV neon sign transformer was plugged straight to 110V AC wall power and the electrodes were attached to the output of the transformer.

Tests were conducted on a flat $1/8^{th}$ inch thick acrylic plate used as the dielectric. Different arrangements of electrode widths and gap between them were tested to try and find the optimum arrangement. A TSI brand digital micro-manometer was used to calculate the induced flow velocity from the plasma discharge. Special pitot probes were made out of glass pipettes extruded using a torch to a thin tube with a small tip. Total pressure was taken as atmospheric and the velocity was calculated using the Bernoulli equation.

CHAPTER FOUR: FINDINGS

The investigation can be broken up into three major sections: First, a two-dimensional CFD model was developed to establish a foundation to compare against. Prior works suggest that many CFD models are highly unreliable for separated flows within a diffuser, so this first investigation was performed to reinforce that assumption and hopefully shed some light on the differences between CFD predictions and the actual situation. The second, and most important, section of the investigation was the experimental tests. These tests were performed on two diffuser models at various conditions. The findings will draw comparisons with the CFD model and offer suggestions for improvement for future studies, as well as some options for the development of an active flow control regime. The last section of the investigation is rather minor. A dielectric barrier discharge plasma actuator was built in an attempt to control the flow separation. In the end the resources were not available for a complete evaluation of the technology offering only a preliminary study on its use.

Computational Fluid Dynamics Model

The CFD model was quite simple, and perhaps a rather crude way of comparing computational results to the experimental results, however, as mentioned previously, the CFD model was produced mainly to point out the shortcomings of the current computational techniques in a high adverse pressure gradient flow such as the separated annular diffuser. Being a simple two-dimensional model a single mesh was used and the solution converged in less than 700 iterations for both Reynolds numbers.

The CFD predictions for the pressure recovery along the OD wall have some striking features, Figure 4.1. The curve for the Reynolds number of 100,000 seems fitting, considering that a large reverse flow region should lower the total pressure recovery it is clear why the slope of pressure recovery decreases through the diffuser. However, the pressure recovery for the lower Reynolds number, 50,000, is actually higher overall than for the larger Reynolds number. The CFD model may not be accurately predicting the separation region at this lower Reynolds, subsequently producing an overall pressure gradient that may be too large. In the end though, the pressure recovery is not large enough to suggest reattachment, which will be more evident later when analyzing the contours of pressure throughout the diffuser. Also, it has been noted by Sovran and Klomp (1967) and Cherry et al. (2008) that the pressure recovery will increase with Reynolds number, opposite of these CFD predictions.

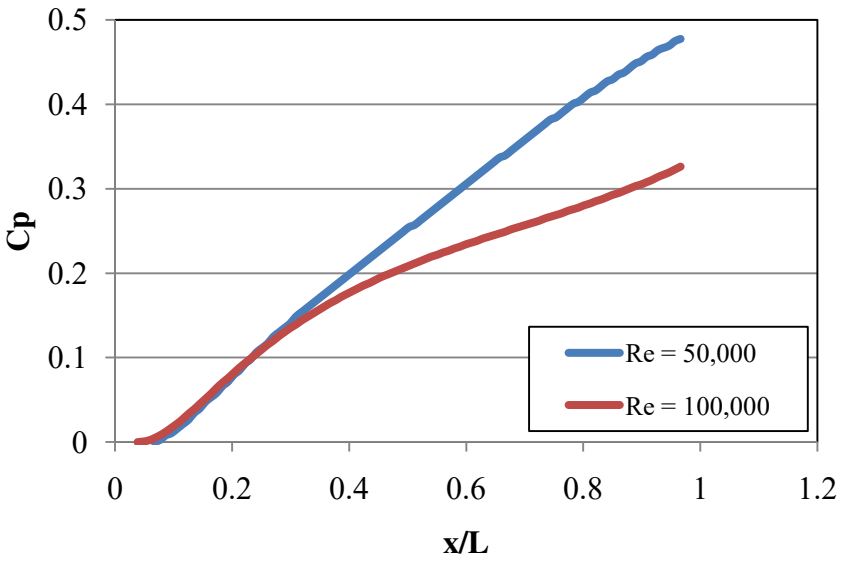

Figure 4.1: Pressure recovery along OD wall from CFD model of diffuser 2

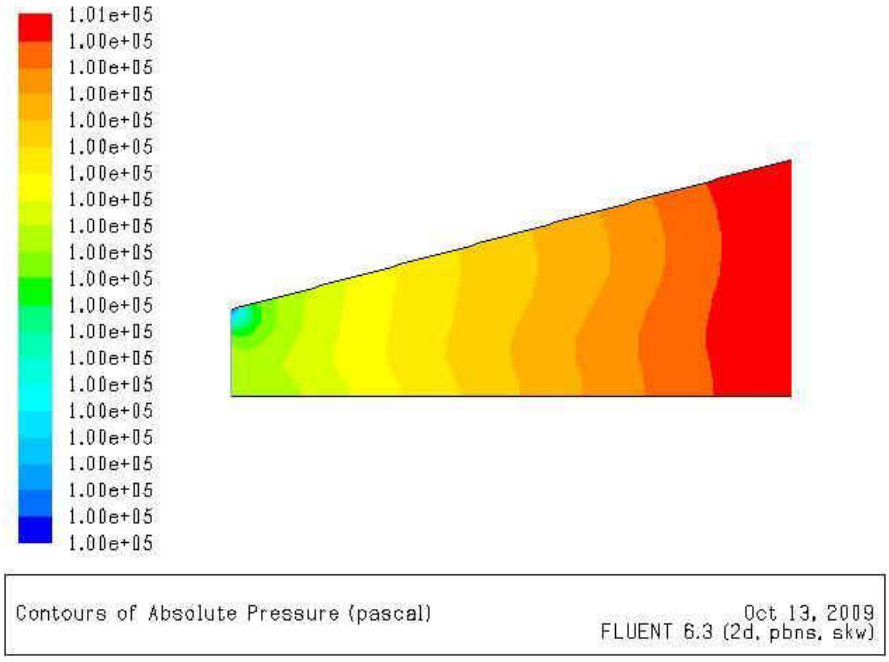

Figure 4.2: Absolute pressure contour at Re =50,000

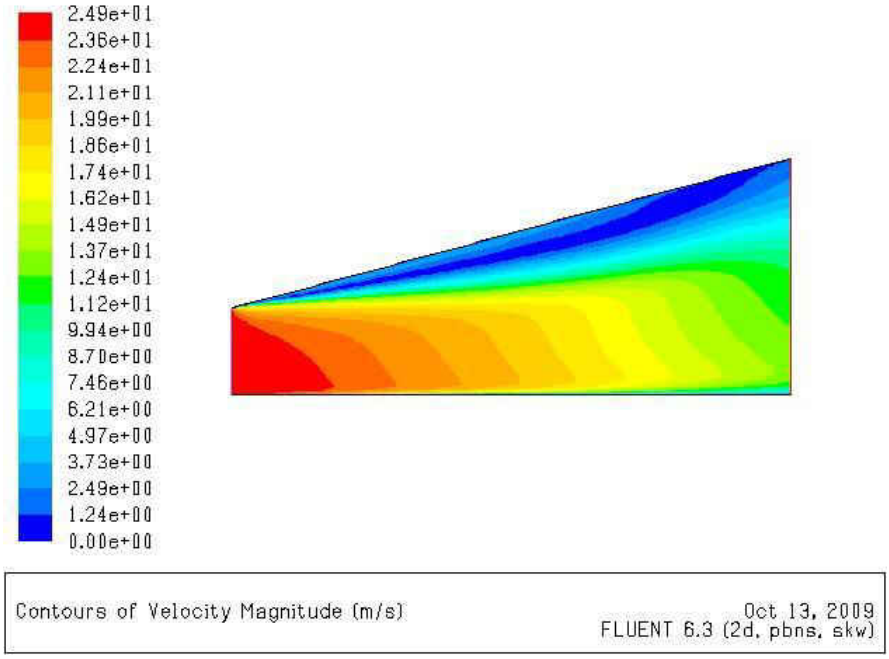

Figure 4.3: Velocity contour at Re = 50,000

Figure 4.2 and Figure 4.3 show the absolute pressure and velocity contours for Reynolds number of 50,000, respectively. The absolute pressure contour validates the constant rise in pressure recovery shown in Figure 4.1, as it is seen to constantly increase moving downstream. There is one location though that may reveal a bit more of what is occurring in this CFD model: the region of low pressure at the OD inlet. Cherry et al. found that the separation point was typically at the corner of the expanding wall, just as the CFD model shows. The velocity contour confirms this. The region of low velocity begins just downstream of the OD inlet point and expands throughout the diffuser. As this region of low velocity grows, as does the adverse pressure gradient, the flow begins to separate, allowing for a region of reverse flow to develop along the OD wall. As seen in the velocity contour, the reverse flow region only grows in the downstream direction, suggesting that the separation never reattaches but instead leaves the wall as a high velocity jet. This region of separation is not too large, however, since the pressure recovery was still quite high.

Looking now at the absolute pressure and velocity contours for the Reynolds number of 100,000 in Figure 4.4 and Figure 4.5, the differences from the lower Reynolds number CFD model can be observed. The pressure rise through the diffuser now is not as large as for the lower Reynolds number, a sign of why the pressure recovery was lower. The region of low pressure at the OD inlet still signifies that the flow is beginning to separate as very early. The velocity contour seems to justify this as well, where the flow velocity drops significantly along the region near the OD wall upon entering the diffuser. The reverse flow region expands at a more rapid pace than for the Reynolds number of 50,000. Since the separation acts as a high velocity jet moving away from the wall there

is a decrease in available forward flow area. This decrease in flow area is so large that the available forward flow area remaining is nearly constant down the length of the diffuser, prohibiting the flow from slowing too much. This realization helps show why the pressure recovery remains so low for this CFD model. Furthermore, from the pressure recovery curve it was shown that the rate of pressure recovery begins to decrease gradually, and by x/L of 0.6 the slope begins to take on a close to linear trend. Cherry et al. (2008) found that for the experimental diffuser this happened a little later on, near x/L of 0.7, and was a sign of the reverse flow region spreading uniformly across the OD wall.

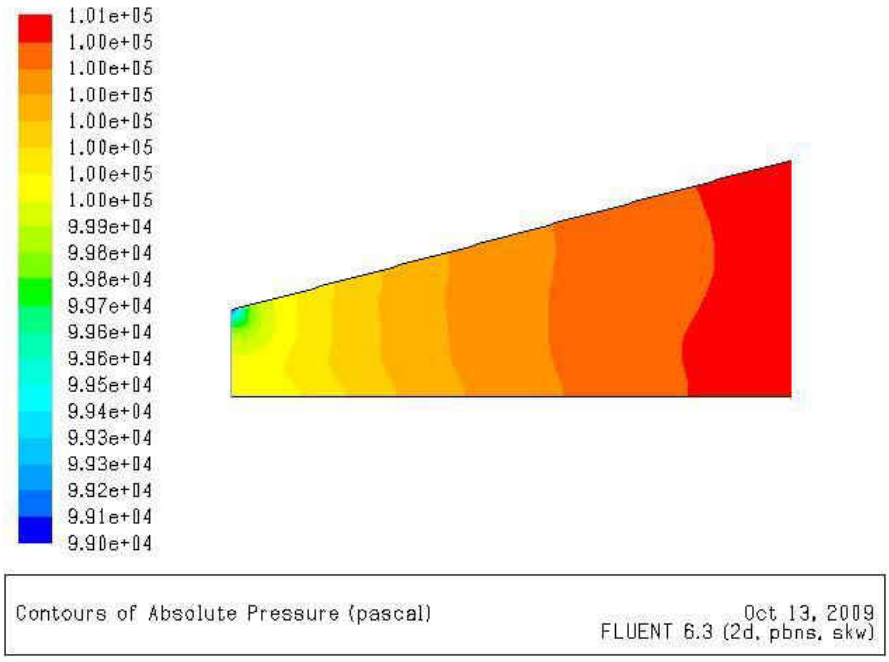

Figure 4.4 : Absolute pressure contour at Re = 100,000

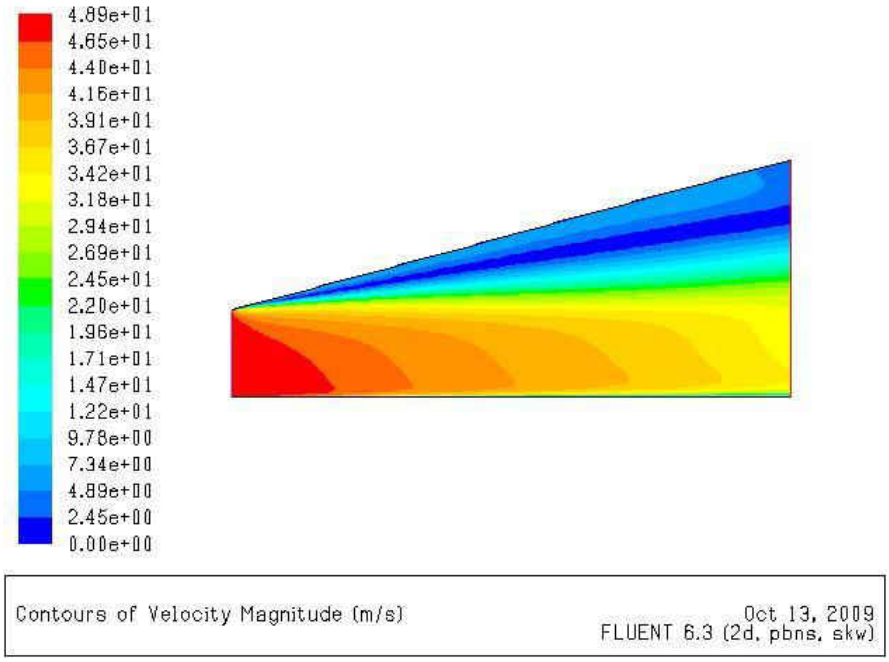

Figure 4.5: Velocity contour at Re = 100,000

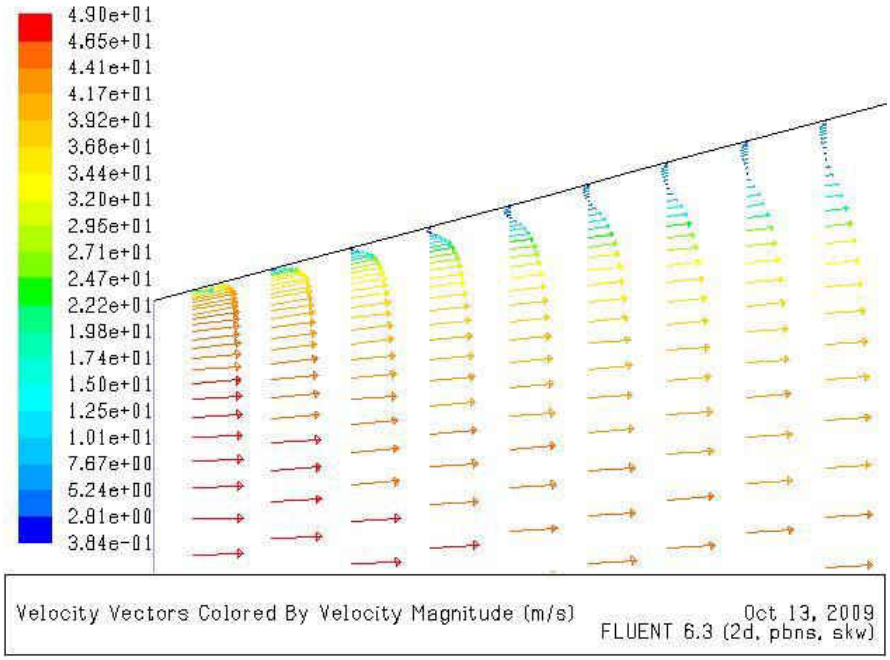

Figure 4.6: Velocity vectors at Re = 100,000 showing the beginning of reverse flow

To give a better idea of what the flow characteristics are like on the OD wall where the separation is just beginning the velocity vectors throughout the diffuser are plotted in Figure 4.6. Starting at the inlet of the diffuser the flow is immediately affected by two mechanisms; first, the "no-slip" condition requires the flow velocity at the wall to be zero and secondly, the affect of the adverse pressure gradient from the diffusions process begins to take over. Within a very short distance along the OD wall the flow velocity can be seen to slowly reverse direction, and spread from the wall in the downstream direction.

Experimental Pressure Data

The majority of the investigation focused on the experimental research on diffusers 1 and 2. And the majority of the experimental research focused on the pressure recovery across the diffusers as a measurable means of studying the flow characteristics of them. The pressure recovery was measured for several cases lending relevance to prior works and to real world industrial applications. These results apply methods used in earlier works studying diffusers in many scenarios, on a rather new area of interest and of little pre-existing experimental data; a three-dimensional annular diffuser. The findings will help shed light on the significance older two-dimensional diffuser data has on the real world case of a three-dimensional annular diffuser.

Separated Diffuser Data

The primary experiments were performed on diffuser 2, the diffuser model with naturally separated flow. Four rows of streamwise pressure taps and three rows of circumferential pressure taps were along the OD wall as well as a series of evenly spaced (every x/L of 0.2) pressure taps along the ID wall were used to collect data. The pressure taps along the

OD wall are tantamount to the arrangement of pressure tap data collected by Cherry et al. (2008). In addition to the numerical data collected tufts were used to visualize the flow separation along the OD wall.

Streamwise Pressure Data

Four rows of streamwise pressure taps were installed to determine whether or not the pressure varied along the OD streamline. If it was found that the pressure did vary then it would have been clear that the flow has quite a bit of non-uniformities, while if it was found that the pressure did not vary much along between rows then it would have allowed for only one row to be used for data collecting. As Figure 4.7 shows, a test was run to measure the pressures for each row. After analyzing the data it becomes quite clear that it is safe to assume that the pressure variation from row to row is negligible.

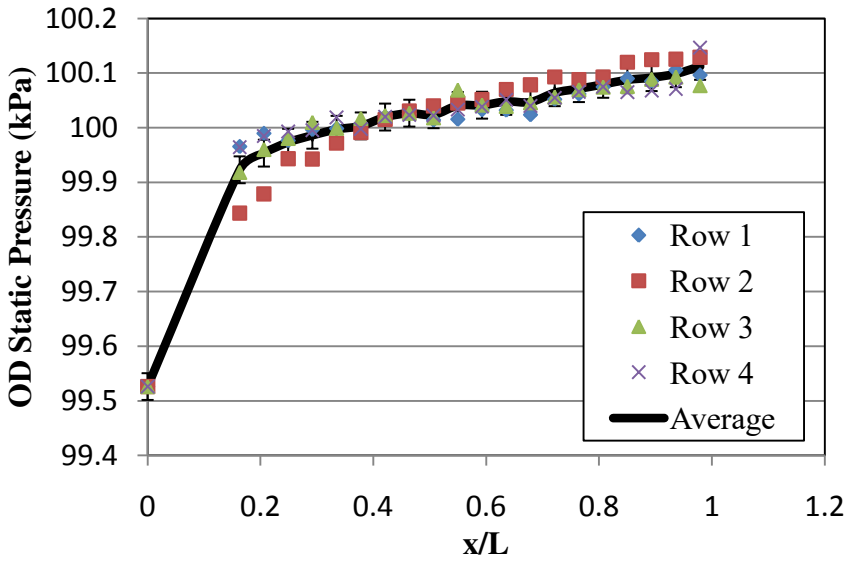

Figure 4.7: Pressure variation between static pressure port rows along outer wall

The average of the four pressure rows shown in Figure 4.7 is seen to lie well within each row measurement, with a statistical uncertainty of +/- 0.025%. The only area where there

seems to be any variation from port to port is in the vicinity at x/L of 0.2. This observation may in fact be foreshadowing to the next discussion on whether or not the OD wall pressure recovery gives evidence as to where the separation begins.

From these observations it was decided to only measure row 1 as it followed the average trend quite well. Hence forth, data was collected on diffuser 2 at two Reynolds numbers, 50,000 and 100,000 for three dump gap ratios,∞, 1.0 and 0.5. Data was also simultaneously collected along the seven pressure taps on the ID wall and at a reference static pressure port just upstream of the diffuser inlet on the OD wall.

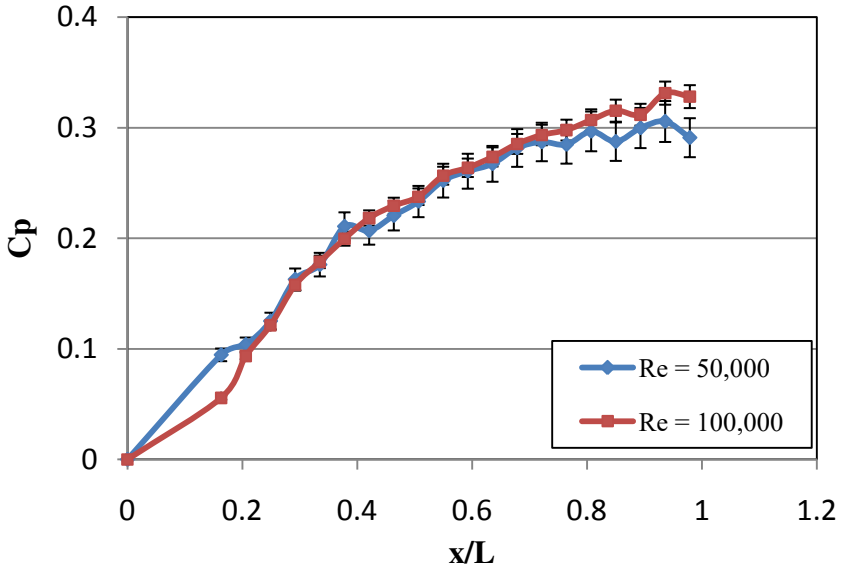

Figure 4.8: Pressure recovery for diffuser 2 OD, dump gap ratio equal to ∞

The first test is the limiting scenario where the dump diffuser is imagined to be infinitely large. A scenario where there is no obstruction downstream that may inhibit or enhance pressure recovery within the CD diffuser. Figure 4.8 shows the pressure recovery at Reynolds numbers, 50,000 and 100,000, for a dump gap ratio of ∞ and a total

measurement uncertainty of 6.06% and 3.16%, respectively. The slope of the pressure recovery is never very steep indicating that separation exists, furthermore, since the pressure recovery slope continues to decrease shows that the separation never reattaches, but more likely remains separated as a high velocity jet away from the wall. Also, we can notice an inflection point at about x/L of 0.2; this location will continue to come up, so keep it in mind.

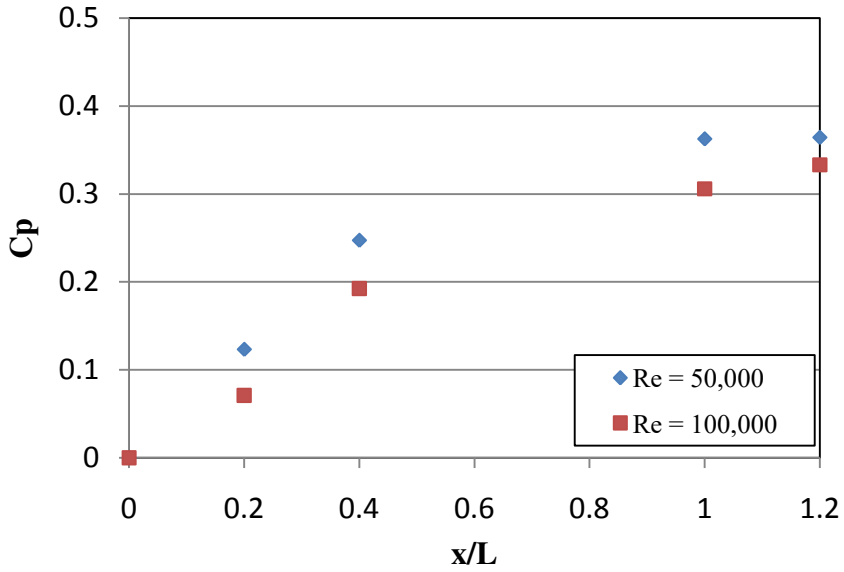

Figure 4.9: Pressure recovery on diffuser 2 ID, dump gap ratio equal to ∞

Figure 4.9 shows the pressure recovery along the ID wall with a dump gap ratio equal to ∞. Plotting the recovery on the ID wall is a less accurate than that of the OD wall purely because of the lack of data points. The lack of volume within the annulus restricted the amount of pressure taps that could be installed. Nevertheless, these measurements were expected to show a fairly constant increase in pressure as the ID wall does little in the work of diffusing the flow. As expected the data shows a steady rise in pressure recovery. Notice also that the values of C_p at each x/L location are consistant with the values found

on the OD wall. This is a general fact for incompressible flow, the static pressure should be the same at all locations at a given cross section. Of course, the total pressure will vary as the velocity increases away from the wall where the *no slip condition* holds.

The inflection point at x/L of 0.2 on the OD wall noticed earlier is much more evident now when the dump wall is in place at a dump gap ratio of 1.0. As seen in Figure 4.10 in the same vicinity of x/L of 0.2 the pressure recovery, while rising steadily, suddenly drops off then begins to increase at a lower rate. Now with the dump wall in place the location of the separation is much more evident, as the wall is clearly influencing the flow upstream. Also, perhaps more importantly, the pressure recovered just prior to separating is more than when no wall was in place. This is supportive of Fishenden and Stevens (1977) who noted that the presence of the flame tube would actually aid in pressure recovery. Notice that for a brief moment following the separation point the pressure recovery actually decreases. For the pressure recovery to decrease momentarily the wall static pressure must also decrease, as it is the only variable in the equation for pressure recovery, Equation 8. But if the static pressure is decreasing momentarily then that would mean that the velocity is actually increasing. The cause for this is the influence of the wall on the beginning region of the separation; the wall is accelerating the reverse flow to an extent that it takes up a large portion of the cross sectional area at the separation point, causing the main flow to increase in velocity through this portion. However, this is short lived as the influence of the main flow pushes the reverse flow back some, increasing the flow area and causing the separation to break away from the wall as a high velocity jet.

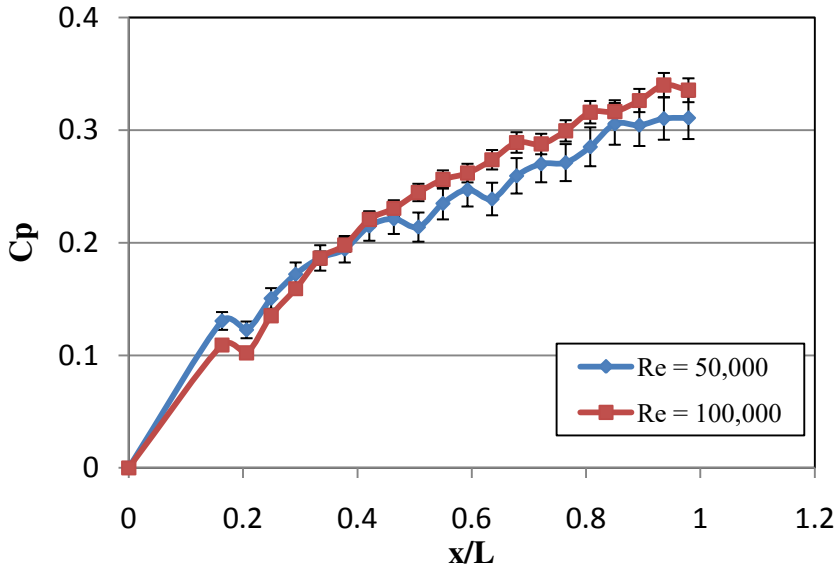

Figure 4.10: Pressure recovery on diffuser 2 OD, dump gap ratio equal to 1.0

Findings by Cherry et al. (2008) suggest that the location where the pressure recovery begins to rise again around x/L of 0.25 at a more gradual slope indicates the location where the reverse flow region has spread uniformly across the expanding wall of the diffuser. Cherry et al. (2008) found reverse flow to makes up 18.5% of the total flow area. As the separation area grows rapidly downstream of this point it begins to counteract the cross sectional area of the diffuser by reducing the area accessible to forward flow. The result of this being a less steep pressure gradient (Cherry et al., 2008).

The impact of the dump wall on the pressure recovery of the ID is very apparent, Figure 4.11. A steady pressure rise can still be seen, but now it is more drastic than when the dump wall was not in place. In fact, a comparison of the C_p value at a given x/L location is larger along the ID wall than it is along the OD wall. This is early evidence of the impact the dump wall has on the uniformity and steadiness of the flow within the CD diffuser. It is also important to note that the pressure continues to rise downstream of the

CD diffuser exit. This is a benefit of the presence of the dump wall on additional pressure recovery within the combustor-diffuser system.

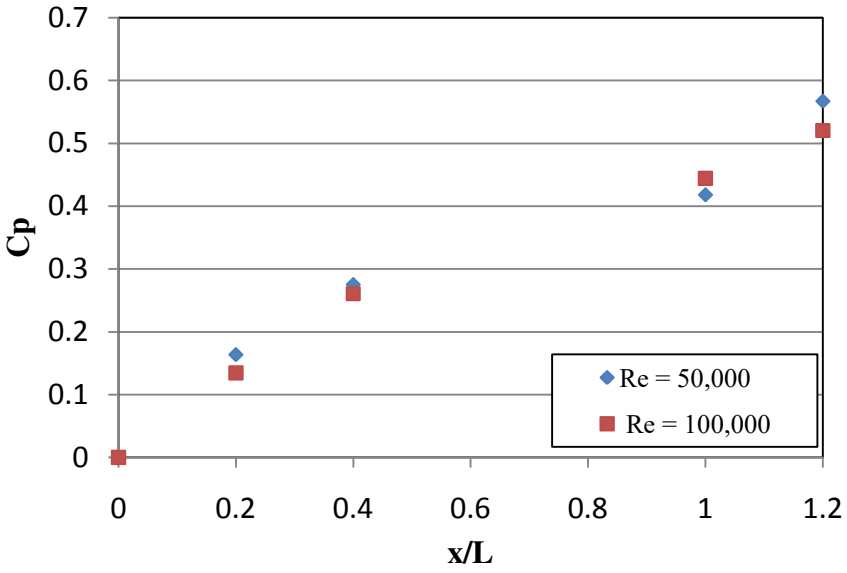

Figure 4.11: Pressure recovery on diffuser 2 ID, dump gap ratio equal to 1.0

We now see what happens when the dump wall is placed too close to the CD diffuser exit. At a dump gap ratio of only 0.5, Figure 4.12 shows an unfamiliar pressure recovery trend. The pressure recovery slope is greater even still up to the inflection point at x/L of 0.2. Now however, there is a more gradual decline of the slope after the inflection point than for the larger dump gap ratios. Though, the slope never regains its positive trend for nearly the rest of the diffuser length and remains close to zero. There is another inflection point by x/L of 0.8 where a very steep pressure recovery is noticed throughout the remainder of the diffuser, giving this configuration the largest amount of pressure recovery. But what is happening for the majority of the diffuser length where the pressure recovery remains constant?

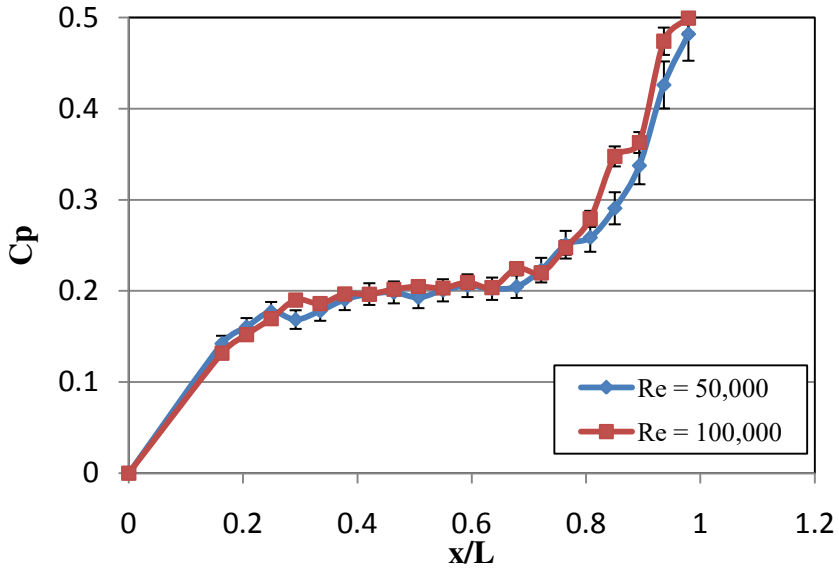

Figure 4.12: Pressure recovery on diffuser 2 OD, dump gap ratio equal to 0.5

The steadiness of the pressure coefficient from x/L of 0.2 to 0.7, followed by a rapid rise in pressure recovery from x/L of 0.7 onward indicates strongly that for this dump gap ratio the separation reattaches, creating a separation bubble. What has happened here is that the boundary surface of the vortex formed just downstream of the ID separation point was influential enough to modify the pressure distribution enough for the flow to reattach, creating a separation bubble. Once again, this is indicative of the findings from Fishenden and Stevens (1977) who noted that the presence of the flame tube could increase pressure recovery in the CD diffuser.

The reason for the nearly constant pressure recovery between x/L of 0.2 to 0.7 is that the separation bubble is occupying more of the cross sectional area than the jet like separation seen prior. The presence of the separation bubble is decreasing the flow area more than when the separation reattaches downstream of the exit. This is perhaps the limiting case described by Cherry et al. (2009) explaining how the rate of pressure

recovery is decreased as the reverse flow area competes for diffuser cross sectional area with the forward flow area. As the reverse flow area occupies more and more of the total area the area for forward flow is decreased, thus making the rate of pressure recovery gentler. Looking at Equation 8, the only variable that changes from point to point is the local static pressure. In the current case, the reverse flow along the OD wall is such that the static pressure does not change in the region of the diffuser where the pressure recovery remains constant. Recall that for the dump gap ratio of 1.0 the affect of the wall was attempting to create a separation bubble that resulted in a decrease in pressure recovery momentarily. Now for the smaller dump gap ratio of 0.5 the affect of the wall was strong enough to influence this reverse flow region to create a separation bubble.

The affect of the dump wall is also very evident along the ID wall. In Figure 4.13 the pressure rise is seen to steadily increase, even though the OD wall exhibited nearly no change in pressure recovery in the region of the separation bubble. Furthermore, the pressure rise along the ID wall is larger than that of the OD wall even before the OD wall saw separation. This is further evidence to suggest that the dump wall is changing the flow significantly within the CD diffuser. The nature of how and why the dump wall is altering the static pressure from the OD wall to the ID wall will be discussed later on after some more findings are made to establish a more thorough understanding of dump wall effect.

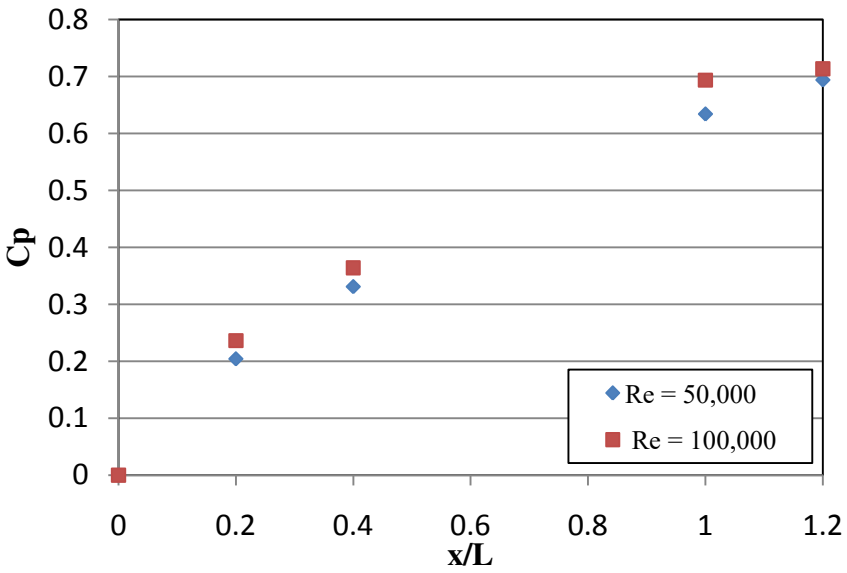

Figure 4.13: Pressure recovery on diffuser 2 ID, dump gap ratio equal to 0.5

Circumferential Pressure Data

Now that a general understanding of the flow separation locations and magnitudes have been found for different Reynolds numbers and dump gap ratios it is necessary to delve deeper into what is happening at these significant locations along the OD wall. To do this circumferential taps were placed at three different x/L locations, 0.2, 0.4, 0.6. Since it was found earlier that the majority of pressure taps in the streamwise direction didn't vary from row to row, it was safe to assume that one 90 degree segment of the diffuser portion could be used for the circumferential measurements.

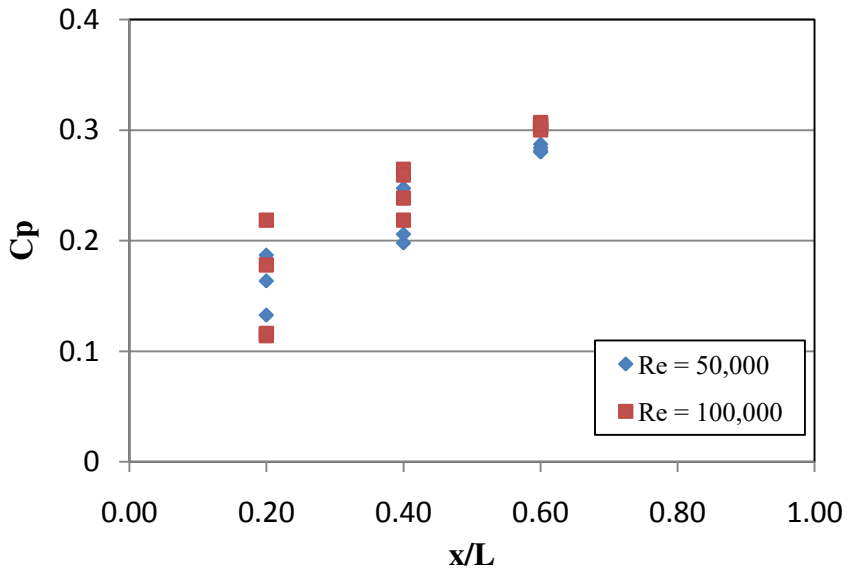

Figure 4.14: Circumferential pressure recovery on diffuser 2, dump gap ratio equal to ∞

It was noted previously that for the dump gap ratios of ∞ and 1.0 the separation was a jet like separation, with a separation point close to x/L of 0.2. In Figure 4.14 the variation for pressure recovery at dump gap ratio of ∞ is shown. Notice how much variation from each pressure tap there is at the separation point, x/L of 0.2. This is a very unsteady location where the main flow is being suddenly redirected by the nose of a reverse flow zone. However, as the reverse flow region begins to establish itself down the diffuser the flow becomes a bit more uniform, seen in a more precise location of pressure recovery points. By x/L of 0.6 each measurment is nearly in the same location, this is suggestive that with the absence of the dump wall the flow exits the diffuser quite unifrmly.

In Figure 4.15, the variation in pressure recovery at a dump gap ratio of 1.0 is seen to be very similar to that of the dump gap ratio of ∞. At the separation point, x/L of 0.2, the variation in pressure recovery is once again very large, as the main flow is disrupted by a reverse flow region. However, unlike the dump gap ratio of ∞, the variation in pressure

recovery is still impactful by x/L of 0.4 and even a bit by x/L of 0.6. The cause is that the presence of the wall is making it difficult for the reverse flow region to spread uniformly across the wall. In Figure 4.10 we can see how bumpy the pressure recovery is, esspcially for the Reynolds number of 50,000, while the same can not be said for the pressure recovery shown in Figure 4.8. Just as noted by Agrawal et al. (1998), it is clear that with the presence of the dump wall the flow will not be uniform upon exiting the CD diffuser.

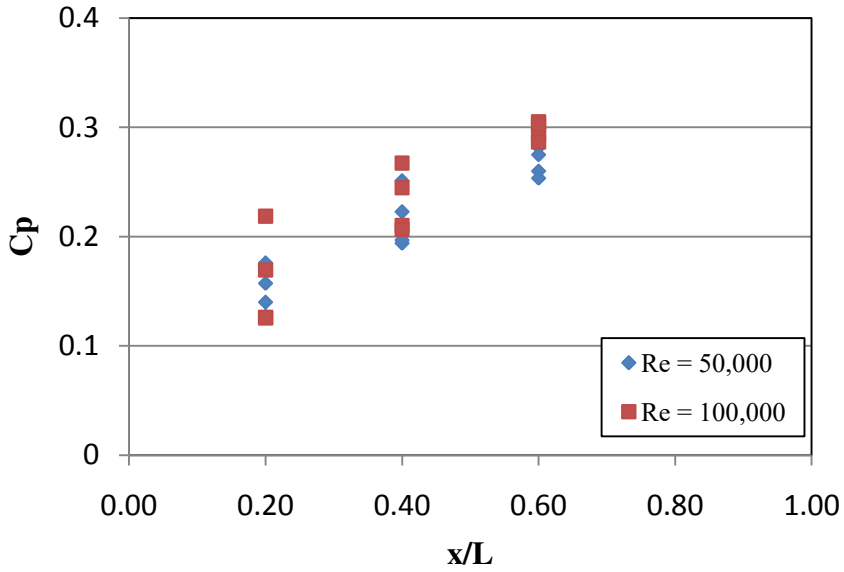

Figure 4.15: Circumferential pressure recovery on diffuser 2, dump gap ratio equal to 1.0

The unsteadiness in the pressure recovery seen in Figure 4.15 is also evidence of the influence of the reverse flow region near the separation point already discussed. Throughout the region where the reverse flow meets the separation point the struggle for a separation bubble to establish, and ultimately fail to do so, is part of the cause for the non-uniformity in the pressure recovery around this location and in the downstream region as well.

A trend reversal in the pressure recovery variation is noted for the dump gap ratio of 0.5, Figure 4.16. Now the variation is fairly low at low x/L and increases closer to the exit. The slight variation in pressure recovery at x/L of 0.2 is evidence of the separation location and the struggle for the reverse flow to guide the main flow. As the separation bubble becomes established and the reverse flow spreads uniformly across the diffuser wall the variation in pressure recovery is very low, this can be seen at x/L of 0.4. By x/L of 0.6 the separation bubble is nearly reattached, which is seen as a variation in pressure recovery once again as the main flow struggles to once again follow the contour of the diffuser wall.

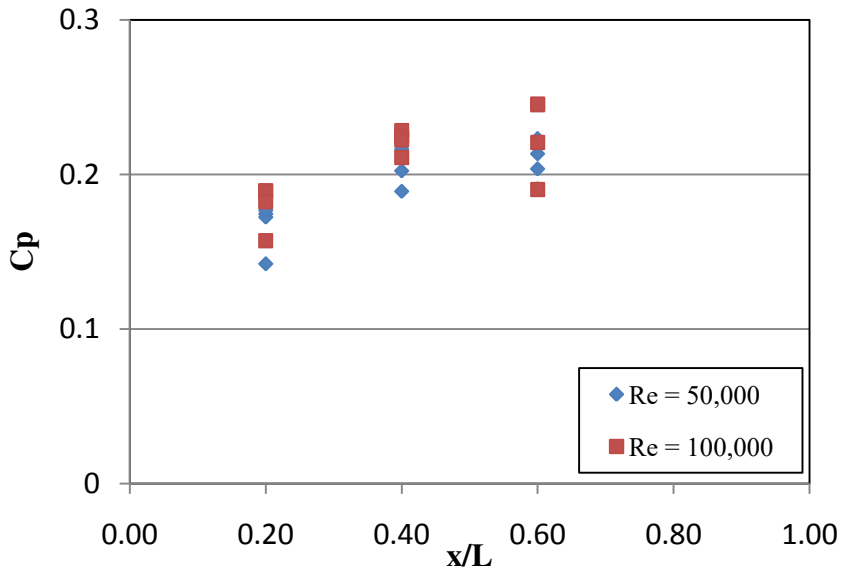

Figure 4.16: Circumferential pressure recovery on diffuser 2, dump gap ratio equal to 0.5

In the end the pressure recovery may be larger at the smallest dump gap ratio, but from Figure 4.16 we see that the flow uniformity actually decreases moving downstream from the separation point. At x/L = 0.4 the circumferential pressure data all falls in the same general area, however at x/L = 0.6 there is quite a larger range that the data falls on. So

there is a careful balance between the desired pressure recovery and the degree of unsteadiness in the flow exiting the CD diffuser. This tradeoff must guide the remainder of the design of the combustor-diffuser system.

Outer Wall Pressure Recover Contours

Evidently the separated flow through a three-dimensional annular diffuser is quite complicated. The flow field along the separated wall is highly non-uniform, varying with the dump gap. The previous results have illustrated this, but to help visualize further, contour maps were created utilizing all the streamwise and circumferential pressure data. The contour maps show the pressure recovery on a one-quarter section of the entire OD wall of diffuser 2.

The pressure recovery contours along the OD wall of diffuser 2 with a dump gap ratio of ∞ for Reynolds numbers 50,000 and 100,000 are shown in Figure 4.17 and Figure 4.18, respectively. In the region where the flow separation leaves the wall as a high velocity jet the pressure contour is very unsteady circumferentially. The reason for this is that the reverse flow experiences non-uniformity when it is being ejected from the wall as a high velocity jet. It is also important to notice the flow behavior at the separation point near x/L of 0.2. For the low Reynolds number the pressure recovery is fairly uniform across the diffuser wall, however at the higher Reynolds numbers the pressure recovery is more unstable. This non-uniformity at the separation point for high Reynolds numbers may propagate downstream, explaining the larger degree of disorder circumferentially compared to the lower Reynolds number across the entire OD wall.

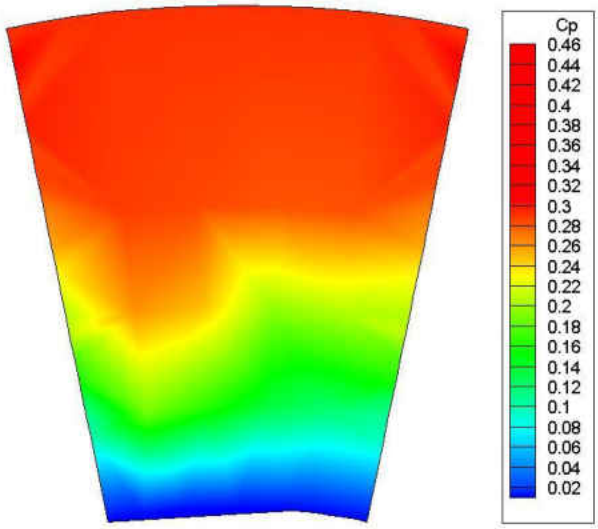

Figure 4.17: Pressure recovery contour on diffuser 2 OD wall, DGR = ∞ Re = 50,000

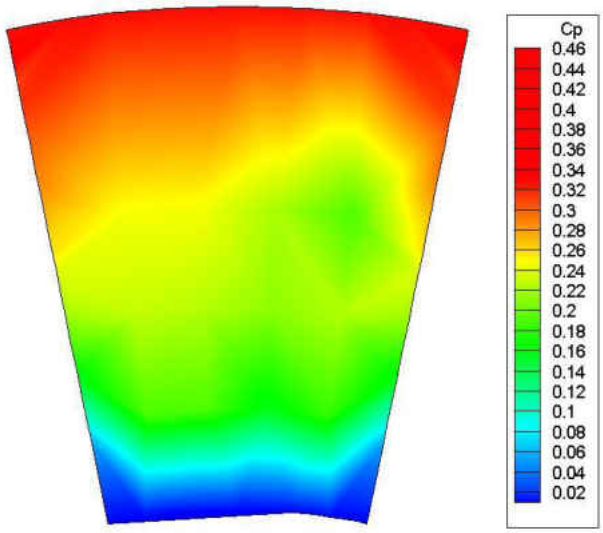

Figure 4.18: Pressure recovery contour on diffuser 2 OD wall, DGR = ∞ Re = 100,000

The pressure recovery contours are very similar at the dump gap ratio of 1.0 compared to the dump gap ratio of ∞. For the lower Reynolds number of 50,000, Figure 4.19, the pressure recovery at the separation point, x/L of 0.2, is nearly constant once again. Moving downstream though, where the reverse flow region is larger, the uniformity across the diffuser wall begins to break down. However, for this low Reynolds number the flow regains uniformity before the diffuser exit, and for the most part is pretty uniform for a good part of the downstream section of the diffuser.

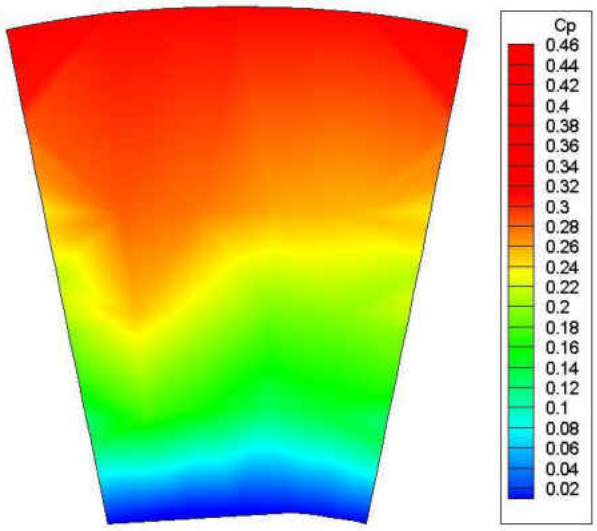

Figure 4.19: Pressure recovery contour on diffuser 2 OD wall, DGR = 1.0 Re = 50,000

Once again, at the larger Reynolds number, 100,000, there is less uniformity in the flow at a dump gap ratio of 1.0, Figure 4.20. The presence of non-uniform pressure recovery near the separation point is seen to propagate downstream throughout the region of reverse flow. The fact that the pressure recovery is more uniform at the separation point

for the lower Reynolds number suggests that the flow is more stable at the separation zone for the lower Reynolds number compared to the higher one. Unlike the pressure recovery contour shown in Figure 4.18 however, the pressure recovery becomes mostly stable near the exit of the diffuser, suggesting that the presence of the wall at this dump gap location has a positive effect on the flow uniformity near the diffuser exit.

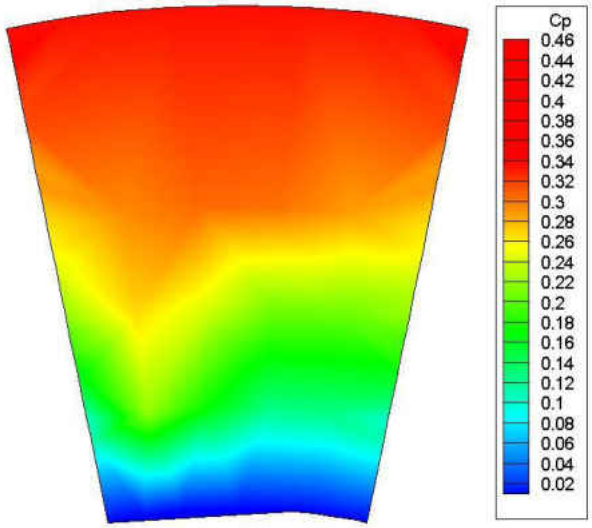

Figure 4.20: Pressure recovery contour on diffuser 2 OD wall, DGR = 1.0 Re = 100,000

The contours of pressure recovery for the dump gap ratio of 0.5 help shed some light on the flow behavior for within a separation bubble, as seen in Figure 4.21 and Figure 4.22. The circumferential data in Figure 4.16 suggested that the pressure recovery was fairly uniform near the separation point at x/L of 0.2, and the contour plots support this. Throughout the region of separation the contour plots remain very uniform and constant, as seen earlier in the streamwise pressure data, Figure 4.12. By x/L of 0.8 the separation

bubble reattaches to the wall and the pressure begins to recover more. In the contour plots this is characterized by a very rapid increase in pressure recovery associated with flow non-uniformities circumferentially. The flow non-uniformities are greater at the Reynolds number of 100,000, which in retrospect, was evident earlier in Figure 4.12 where the rise in pressure recovery near the exit of the diffuser was jagged for the higher Reynolds number. So, in regions of large pressure recovery, it can be expected to also find a large degree of non-uniformities in the flow across the surface seeing separation. A drawback to having the dump wall too close to the diffuser exit can also be found here: While the extent of the flow for the dump gap ratio of 0.5 is very uniform, the region of the flow that is not very uniform is found too close to the diffuser exit. This creates an unfavorable flow regime for the dump diffuser and will complicate design criteria.

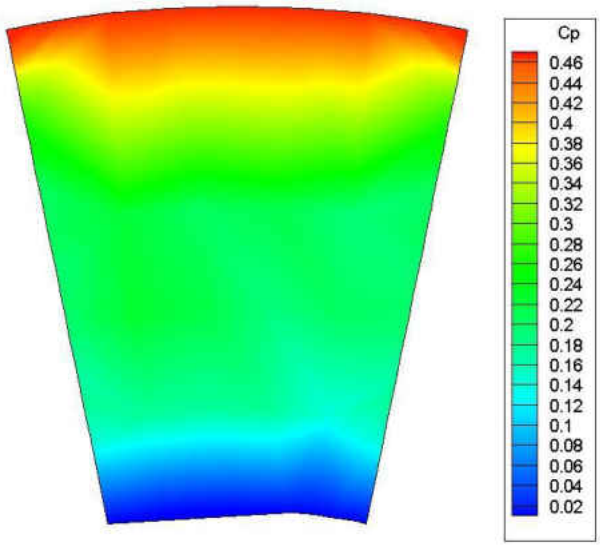

Figure 4.21: Pressure recovery contour on diffuser 2 OD wall, DGR = 0.5 Re = 50,000

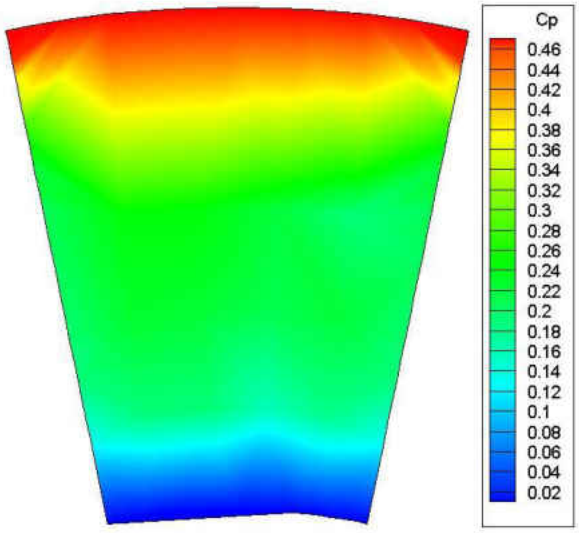

Figure 4.22: Pressure recovery contour on diffuser 2 OD wall, DGR = 0.5 Re = 100,000

Attached-Flow Diffuser Data

To help with the flow characterization of the separated diffuser another diffuser, with naturally attached flow, was studied. Diffuser 1 was made to replicate the General Electric 8362 turbine CD diffuser as outline by Sovran and Klomp (1967). Only one row of streamwise static pressure ports was installed. This was acceptable because it was shown with diffuser 2 that the flow was uniform except in areas of flow separation, and since this diffuser is known not to separate, it was safe to assume that one row of ports would suffice. The data, which was collected under the same conditions as for diffuser 2, helps uncover the differences in the flow behavior between a typical industry diffuser and that of one with low pressure recovery due to separated flow.

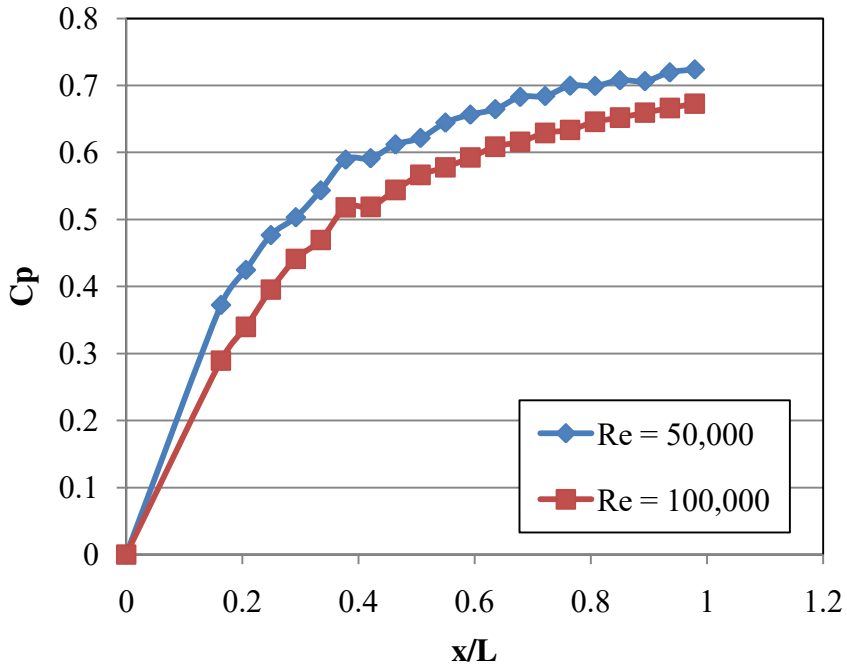

Figure 4.23: Pressure recovery on normally attached diffuser 1

The impact a well designed diffuser has on pressure recovery is very evident when looking at the recovered pressure for diffuser 1 in Figure 4.23. For both Reynolds numbers the total pressure recovered is well above 0.6, with a very steep slope from x/L of 0 to 0.4. Both Sovran and Klomp (1967) and Cherry et al. (2008) note that the pressure recovery rises with a rise in Reynolds number; however this is not the case for these results. While the pressure rise through the diffuser at the higher Reynolds number is larger than that for the lower Reynolds number, the effect the velocity has on the pressure recovery over powers the pressure rise. The smaller pressure rise attributed to the smaller angle diffuser can help explain this. From equation 11, the ideal pressure recovery, neglecting the decrease in total pressure through the diffuser is 0.852. The diffuser effectiveness, explained in equation 12, shows that for both Reynolds numbers the diffuser effectiveness is quite good, 0.842 for the Reynolds number of 50,000 and 0.802

for the Reynolds number of 100,000. These calculations are explained in detail in Appendix D.

Flow Visualization

Two flow visualization techniques were employed in this study; smoke and tufts. A fog machine supplied the smoke, but unfortunately the post processing of the video data was not clear enough to present in this thesis. However, the data from the tufts is very clear and makes a good example of the experimental results already discussed. Two tests cases were run with the tufts, one with the dump wall at ∞ and one at 0.5, both at a Reynolds number of 100,000. These two cases were chosen because by the experimental results they should show two very different flow fields; one with a separation leaving the wall as a high velocity jet, and the other as a separation bubble that reattaches within the diffuser.

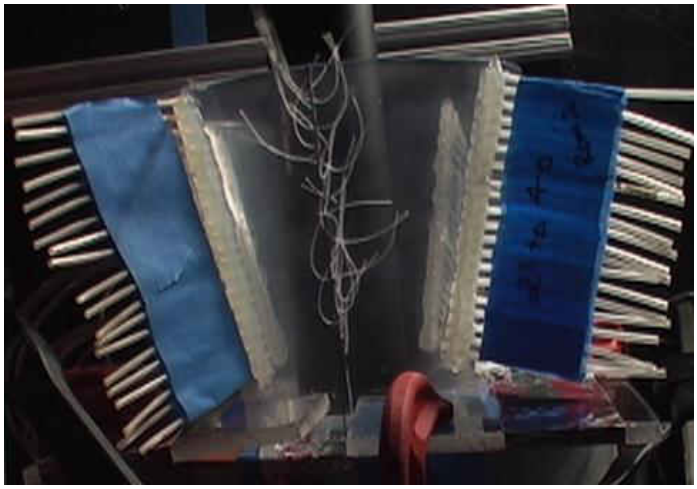

Figure 4.24 : Tufts on diffuser 2 with dump gap ratio of ∞

A snap shot of the tufts on the OD wall of diffuser 2 with a dump gap ratio of ∞ and a Reynolds number of 100,000 is shown in Figure 4.24. Recall that for this arrangemetn in

the experimental data a large portion of the OD wall was covered in very non-uniform reverse flow that separated as a high velocity jet away from the wall. This can be seen in image of the tufts, as each tuft seems to be pointing in a different direction. What this image does not reveal is that each of these tufts were constantly circulating and moving back and forth, none following the same course as another. This reinforces the notion of a highly non-uniform reverse flow region. In fact, most of these tufts were turning back and pointing upstream as it was caught in the reverse flow. Also, notice that the tufts exiting the diffuser are still non-uniform, showing that the flow remains separated throughout the diffuser.

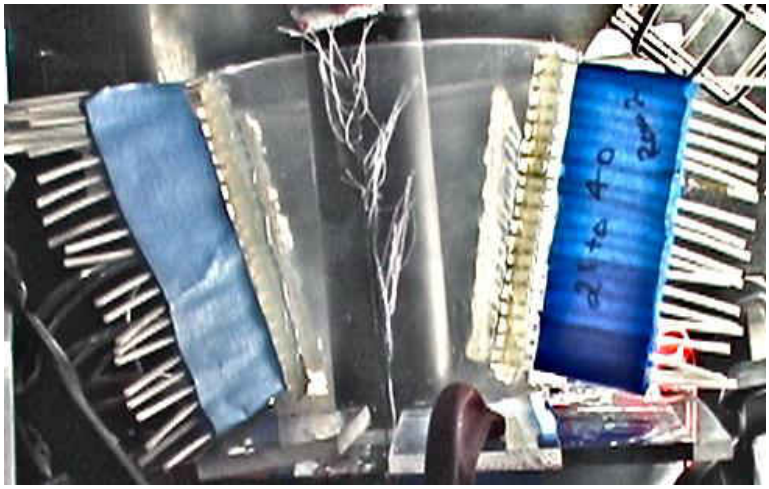

Figure 4.25: Tufts on diffuser 2 with dump gap ratio of 0.5

The tufts acted quite different when the dump gap ratio was set at 0.5, as seen in Figure 4.25. It was suggested earlier that the separation bubble was more uniform than the jet-like separation at larger dump gaps, and this is apparent with the tufts. The tufts are, for the majority, following the streamwise direction, very much so in the first half of the diffuser. Some distortion in the tufts is witnessed near x/L of 0.6, which was also seen in

the circumferential data. Also, the tufts exiting the diffuser are aligned with the streamwise direction. What is more interesting is that the tufts take a sharp uniform 90 degree turn out of the diffuser exit by the impact of the wall being so close. This helps explain the process the wall has on forcing the separation to be a bubble within the diffuser. With the wall so close, its presence is transferred upstream to allow the flow to be redirected well before reaching the wall.

Plasma Actuator Discharge Performance

All the work presented thus far was an attempt at characterizing the separation phenomena within an annular diffuser; this final section of findings will go over initial attempts at controlling this flow separation. A dielectric barrier discharge plasma actuator was built and several scenarios were tested for different electrode and electrode gap arrangements. Initially, tests were conducted on a flat 1/8 inch sheet of acrylic following the electrode placement strategy of Singh and Roy (2008) and the measurement technique of using a glass pipette pitot probe to measure the total pressure within the plasma wind. These tests included the variation in top and bottom electrodes and the gap between them. Even though the plasma actuator rig was not ideal, a measurable velocity was found within the plasma field. The average 1.68 m/s while the maximum velocity was 2.91 m/s at a top electrode width of 2 mm, a bottom electrode width of 4 mm and an electrode gap of 2 mm. This arrangement is similar to the arrangement used by Singh and Roy (2008), the only difference being that the bottom electrode width in that experiment was 2 mm not 4 mm.

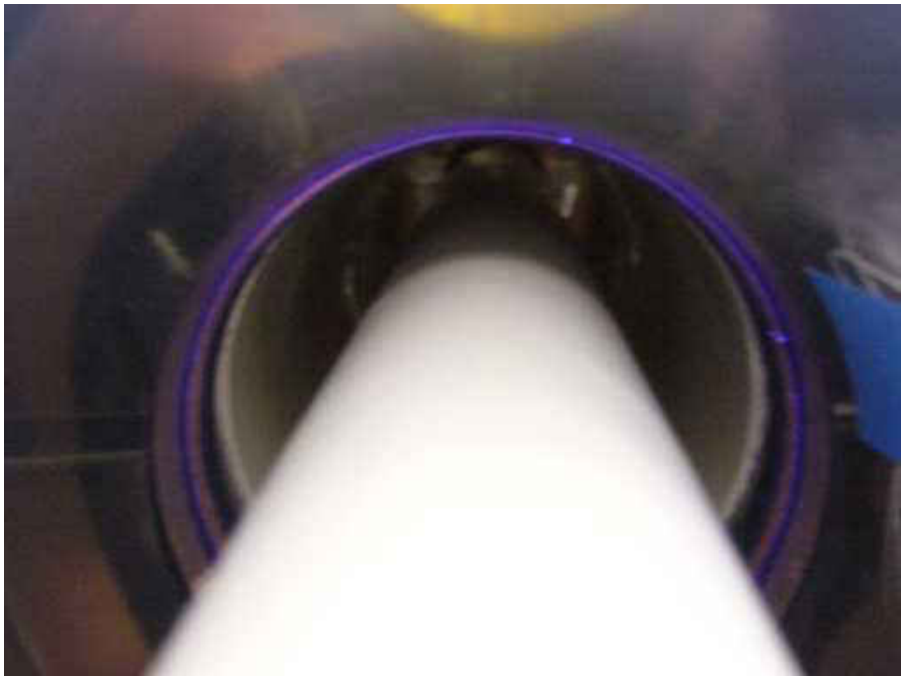

Figure 4.26: Plasma discharge on diffuser at x/L = 0.2

Once these initial measurements were taken to understand how to control the plasma discharge, it was desired to impliment the DBD actuator within the diffuser. The electrode arrangement that yeilded highest plasma velocity was used for the diffuser tests. Furthermore, the electrodes were positioned at the approximate separation point, x./L of 0.2. Figure 4.26 is an image of the ring of plasma during a test, looking up the diffuser from the exit plane. The technique for creating and controlling the plasma worked very well, and it can be seen that the plasma field is quite uniform and dense, even though the amplifier was not used in the DBD actuator rig. A row of tufts was placed on the OD wall in which a somewhat noticeable effect of the plasma was recorded. During a specific test a few tufts located with the zone of x/L from 0.2 to 0.5 were stuck on the wall, perhaps by friction. But as soon as the plasma was turned on, which energized the boundary layer,

the tufts became un-stuck and followed the contour of the steamline near the wall. This is very suggestive evidence that this same effect could decrease the chance for a separtion point to develop along the diffuser wall. Prior work by Singh and Roy (2008) and Corke et al. (2009) among others, have suggested that the effect of plasma on separation control may not be very applicable at the high speeds found in the turbomachine. However, the tests demonstrated here show an appreciable impact of the plasma on the separation within the annular diffuser, even at substantially high flow velocities. It is most agreeable that the plasma affects the energy balance within the inner part of the boundary layer, which reduces the chance for separated flow. However, this effect would be limited at higher flow velocities, where the impact of the added energy may not be considerable enough to prohibit flow separation. The reason that the plasma is able to reduce the flow separation at the higher velocites than previously expected may very well be that not only does it affect the energy balance, but also the *no slip condition* at the wall. In fact, this may play an even larger role in the plasma affect on the flow. With the aid of the plasma discharge the flow will see a moving wall conditions rather than the stationary wall. This will of course deminish the adverse pressure gradient responsible for the separated flow.

Discussion of Findings

The results presented in this investigation have help uncover some of the complexities associated with separated flow in an annular diffuser, specifically the impact the downstream dump wall has on the flow in the upstream CD diffuser. To evaluate these findings for their legitimacy a few points of interest need to be discussed. First, a comparison of these findings should be made with empirical, or otherwise, widely

accepted data. This means comparing the pressure recovery from the current experiments to that of early experiments that the majority of today's diffuser research is based off of. Secondly, once a clear physical understanding of the flow is revealed, making sure that the results are valid, a comparison to the computational fluid dynamics model can be made. This comparison will help shed some light on the issue of CFD prediction accuracy for separated flows, and perhaps help lead future studies in the right direction for developing more robust CFD models. Once these two steps are finished, and the results can be trusted, some key observations of the flow characteristics found during the investigation should be brought to light.

There are a few early studies that represent the foundation for the majority of later studies on annular diffusers. The work by Sovran and Klomp (1967) stand out as one work that many others were later based off of. The work done by Adenubi (1975) and later re-discussed by Wilson (1984) tested a diffuser model very similar to those on diffuser 2. Adenubi plotted pressure recovery for an annular diffuser with a diffusion angle of 15 degrees at a Reynolds number 120,000, which is reprinted in Figure 4.27 along with the experimental data for diffuser 2 at a Reynolds number of 100,000.

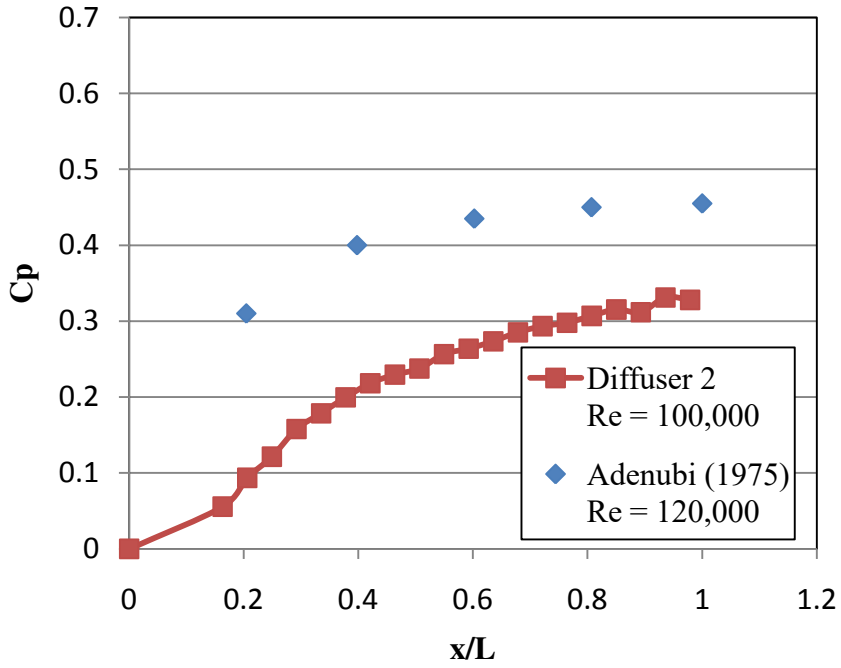

Figure 4.27: Comparison of OD wall pressure recovery on diffuser 2 with findings from Adenubi (1975)

Interestingly, the Adenubi data seems to follow the same trend as the experimental data, but with a larger degree of pressure recovery. So what would cause the two experiments to be off? The cause behind this can be understood very well by a description from Sovran and Klomp (1967), in which it was noted that large diffusion angles produce lower recovery, with the effect being the largest for small area ratios. This comes as a consequence of the large streamline curvature required to turn the flow from the axial direction to the direction along the wall. With a small area ratio there is a larger amount of wall length in this region where the flow direction is still being turned. Furthermore, the tests by Adenubi were run at slightly higher Reynolds numbers, but with a much smaller hydraulic diameter at the diffuser inlet, meaning that the inlet velocity was much larger. Now, although the testing conditions do not match entirely, there is still some

validity in this comparison, as it represents the common trend of pressure recovery for this wide of an angle diffuser. Accordingly, this comparison was a means to assert that the pressure recovery trend was valid, which it can now be assumed to be.

Assuring that the experimental data fit with the results from previous works allowed for the results to be trusted. The next comparison that could be made was how these results fit with the computational models. Now remember, previous work has shown that CFD model predictions have a very hard time with the predictions under unfavorable pressure gradients.

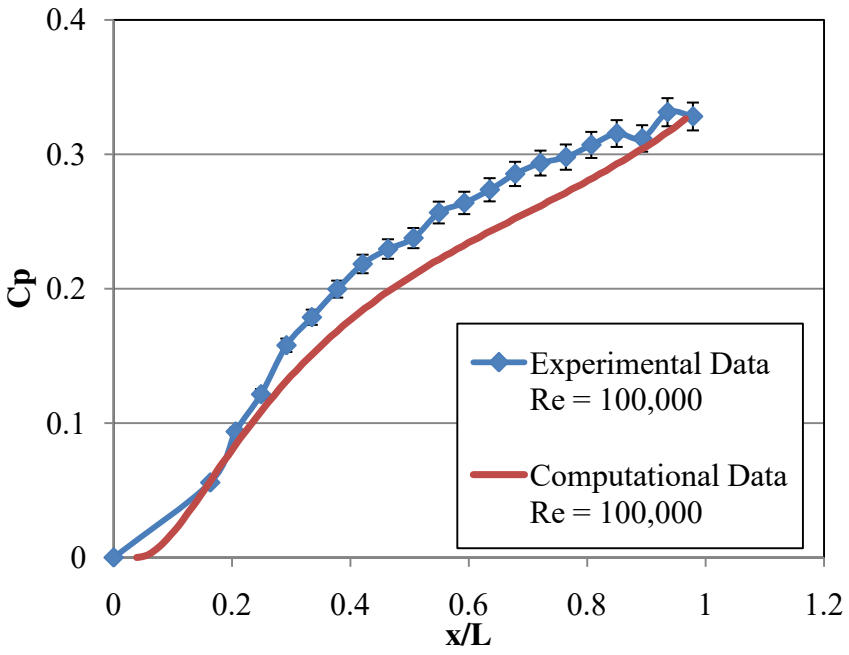

Figure 4.28: Comparison between diffuser 2 pressure recovery and computational results, both at Re = 100,000

A look at the pressure recovery for both the experimental data on diffuser 2 and the computational data each at a Reynolds number of 100,000 shows that the CFD model has actually made a pretty accurate prediction, Figure 4.28. The total pressure recovered is

nearly identical and the trend is nearly the same throughout the diffuser. So what may be concluded here is that there are indeed some CFD models that can decently predict some of the characteristics of separated flow, but this needs to be taken with a grain of salt. The same CFD model was not accurate at predicting the lower Reynolds number flow, suggesting a lower limit in Reynolds number in which the model is accurate. A CFD model should never be used to predict a flow situation without a prior understanding of the flow through experimental or numerical tests.

These supportive findings can assure that the results are accurate. Earlier works show similar trends in pressure recovery, and the CFD model was accurate in predicting one of the flow cases. So now, to answer the remainder of the goal set out with this research, it is needed to explain how this knowledge of the separation characteristics of the diffuser can be used to create an adaptive flow control mechanism. In fact, drawing some comparisons between the experimental results and that of earlier works can help explain some of the flow details.

For instance, Cherry et al. (2008) noted that the separation distributed unevenly across the expanding wall. The experimental data also showed this, as the circumferential measurements were not uniform across a specific x/L value. What this helps show is that in the regions of the diffuser where the circumferential data was not uniform the flow separation had yet to spread evenly across the diffuser. Which means that for a dump gap ratio of ∞ and 1.0 the early regions of the separation zone are not very uniform, with it being more severe for the dump gap ratio of 1.0. The underlying principle to this is that by the nature of the separated zone, it will be very unstable. The flow reversal along one

side of the diffuser wall may not be exactly identical to the reversal on the side annular-opposite* to that point. However, it was noted earlier that some of these flow non-uniformities found near the inlet of the diffuser may be repercussions of small irregularities in the experimental rig upstream of the diffuser inlet. The probability is quite large that the flow was tripped upstream of the diffuser inlet causing the separation region to be non-uniform. This should not be thought of as a problem though because the same likely hood of the flow tripping in a real turbomachine is just the same. What should be taken from these findings is the impact the dump wall has on the natural flow distortions created upstream of the diffuser inlet. It was shown that the severity of the non-uniform flow region near the diffuser inlet was reduced when the dump wall was closest to the diffuser exit. This suggests that the dump wall location is influential on adjusting the flow distortions created upstream of the diffuser inlet.

One surprising difference the experimental results had with previous works is that the pressure recovery difference between the two Reynolds numbers tested was not very large. Cherry et al. (2008) found that the total pressure recovered increased with an increase in Reynolds number, which also supports the earlier findings of Sovran and Klomp (1967). What is interesting is that the current work found a very small rise in pressure recovery for the larger Reynolds number over the smaller one. There are perhaps a few reasons that this has happened. Sovran and Klomp (1967) tested at a Reynolds number 6 times higher than the highest one tested in thesis investigation, 600,000, varying tests by larger Reynolds number increments will make the variation between

* annular-opposite: referring to a point within the volume of the diffuser which is both equal distance radially and 180 degrees in the annular plane from another point.

pressure recovery and Reynolds number more evident. Cherry et al. (2008) ran tests in water tunnel and on a rectilinear diffuser, not an annular one, which makes the Reynolds number significance quite different, as the hydraulic diameter is not the same.

For all the experimental tests it was shown that the majority of the pressure recovery happens early on within the diffuser. For the tests on diffuser 1, where the flow remained attached, the majority of the recovered pressure happened before x/L of 0.4. For the tests on diffuser 2 the flow separated much before this point, around x/L of 0.2, but the majority of the recovered pressure still happened before the separation point. The point to be made is that a separation of the flow early on within the diffuser will be the most drastic on pressure recovery. If the plasma technology can be applied near the separation zone of the diffuser, there is a possibility for dramatic improvement in pressure recovery, even if the plasma does not completely stop the flow from separating. In the worst case the plasma will merely push the separation point downstream, allowing the area of maximum pressure recovery to see attached flow, and gain this recovery. In the best case, of course, the plasma will energize the boundary layer enough to keep the flow from separating at all.

However, pushing the separation point further downstream can create some unwanted results. It was seen that for the dump gap ratio of 0.5, where the separation reattached within the diffuser, the flow was most non-uniform at the diffuser exit. The reattachment point can have just as much a drastic impact on flow uniformity as the separation point has upstream. The test with no dump wall in place showed the most uniform flow at the diffuser exit.

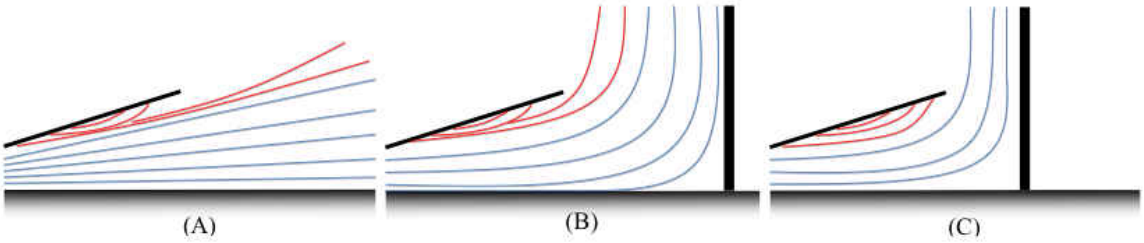

Figure 4.29: Schematic of flow streamlines and separation zone within the diffuser at different dump gaps

So what exactly is happening to the flow with and without the presence of the dump wall that is making such a difference on the flow characteristics? To understand this one needs to recall from fluid mechanics the simple problem of a jet impinging on a flat plate, as this is quite synonymous of the flow from the diffuser coming in contact with the dump wall. Three scenarios are depicted in Figure 4.29, representing the three dump gaps tested. In Figure 4.29 (A) the dump gap ratio is set at ∞, so the flow exiting the diffuser has nothing downstream that will cause it to be redirected. The streamline directions are completely dictated by the geometry of the diffuser itself where the region of reverse flow, and its accompanying jet-like separation, cause a shift in streamline direction.

However, when the dump wall is introduced to the system the flow has to become redirected. In Figure 4.29 (B) the dump gap ratio is set at 1.0, and since the flow is incompressible, the presence of the dump wall travels upstream (by molecular interactions) to allow the flow to compensate for it, just like with the jet impinging on a flat plate. The streamlines compensate for the upcoming dump wall by turning upon leaving the diffuser exit, included in this streamline "re-direction" is the re-direction of

the separated flow as it exits the diffuser. At some dump gap the wall will be close enough for the streamline re-direction to actually "push" the separated streamline back to the OD wall, causing it to reattach.

At the dump gap ratio of 0.5, Figure 4.29 (C), the flow has already become reattached due to the streamline re-direction, with the dump gap small enough for the re-attachment point to be well enough upstream for more pressure recovery to occur before the exit of the diffuser. In this case the streamlines close to the OD wall will make a sharp 90-degree turn at the diffuser exit, which was noticed in the tuft image earlier.

It would be desirable to determine the impact the dump wall has on the curvature of the flow. This is a relatively simple exercise in manipulating the Bernoulli equation for radial flow as shown in Equation 16.

$$\frac{dp}{dr} = \rho v^2 \qquad \text{Equation 16}$$

Integrating Equation 16 gives:

$$p_2 - p_1 = \rho v^2 \ln\frac{r_2}{r_1} \qquad \text{Equation 17}$$

where location 1 is at the diffuser exit plane on the OD wall and location 2 is at the diffuser exit plane on the ID wall. We can designate the radius ratio as R. Solving for R gives:

$$R = \exp\left(\frac{\Delta p}{\rho v^2}\right) \qquad \text{Equation 18}$$

To estimate the radius ratio, R, from the experimental tests we must first estimate the velocity at the diffuser exit. Assuming that the velocity is the same across the exit plane, the ideal velocity can be calculated from continuity using the diffuser inlet velocity and area ratio. Doing such, the velocity at the exit plane was found to be 11.9 m/s and 6.04 m/s for Reynolds number of 100,000 and 50,000, respectively. Using these velocity values and the measured pressure difference between point 1 and point 2 the radius ratio was found to be $R_{0.5} = 1.88$ and $R_{1.0} = 1.55$ at a Reynolds number of 100,000, where the subscript in R represents the dump gap ratio. For the Reynolds number of 50,000 the radius ratios were found to be $R_{0.5} = 1.25$ and $R_{1.0} = 1.17$. As it was probably suspected, the radius ratio is larger at the smaller dump gap than the larger dump gap at the same Reynolds number. This helps reinforce the explanation of how the dump wall can aid the separated flow reattachment. Furthermore, the larger Reynolds number flow sees larger radius ratios, suggesting that there is more curvature of the flow at the higher flow velocities.

Fishenden and Stevens (1977) found that the presence of the flame tube would aid in pressure recovery, and now it is clear why: The flame tube head will cause the re-directed main flow to hinder the ability of the separated flow to exit the diffuser. But there is a drawback to allowing the flow to become re-attached so late in the diffuser; the flow at the diffuser exit becomes non-uniform. It is not an easy process for the dump wall to manipulate the separated flow in such a way, and so there is a constant struggle for the flow to reattach. Many studies suggest that a precise adjustment of the dump gap could be all that is needed to gain sufficient performance from the CD diffuser, but not much effort is put into characterizing the drawback this creates in diffuser exit flow distortions. The

dielectric barrier discharge plasma actuator can eliminate the need for the flame tube head placement to be based on upstream pressure recovery, and thus would allow the flame tube geometries to be dominated more by the creation of a better combustion environment. This idea also applies for the can-annular combustor-diffuser system. With the aid of plasma flow control the dump diffuser geometry can be more orientated towards moving the air to the combustion liner and cooling slots, and less orientated with reducing the air velocity.

The work presented in this thesis has become the initial tests of flow separation at the Center for Advanced Turbines and Energy Research (CATER) at the University of Central Florida. To create a basis for continuation it is necessary to explain the possibilities of future studies on flow separation and separation control. There are three potential areas of interest that can create a good platform for continuation on this research. The first step to be studied should be the application of the annular diffuser within a water tunnel rig that is currently under construction here at CATER. Like the work by Cherry et al. (2008), a water tunnel can be very beneficial in studying separated flow, especially those at turbomachine operating conditions. Reynolds number matching with turbine operating conditions can easily be achieved at low flow velocities within a water tunnel due to the much larger density of water compared to air, about one thousand times greater. The water tunnel also allows for easy flow visualization techniques, among them being dye streaks or hydrogen bubbles created by passing a current through a thin wire in the tunnel. The other two studies may be carried out either in the water tunnel or in the normal air rig: First, a study should be made at more dump gap ratios to quantify more intensely the impact the dump gap has on the flow separation and reattachment.

Furthermore, the dump wall should be fabricated to be more replicable of the dump region in the can-annular design as well as the flame tube in the annular combustor design. These tests will give more reasonable results towards true turbine conditions. The last study needed involves the use of a mechanism to create compressor discharge conditions so that the flow entering the CD diffuser is more replicable to turbine conditions. This mechanism should be capable of generating the swirl typically found at the exit of the compressor as well as any other flow instabilities that may arise from support struts or other flow obstructions found within the turbine in this region.

With these suggestions for future work the understanding of the flow phenomena within the separated annular diffuser will be greatly enhanced. In addition to these initial works more effort needs to be made on the flow control front. The plasma tests presented in this thesis have shown promise to its use in flow control. More work now needs to be performed using DBD plasma discharge on the annular diffuser with a more sophisticated plasma actuator setup. Doing such can help create a better understanding of the way that plasma is aiding in separation control and hopefully backup the assumption made here that the *no slip condition* is affected by the plasma discharge.

CHAPTER FIVE: CONCLUSIONS

The diffuser is a component found in all turbomachines and is used to decrease flow velocity while increasing fluid pressure. As geometrically simple as the diffuser may be, it is actually a quite complex aspect of the turbine. Flows with high adverse pressure gradients produce many problems in modeling and design. Prior research has shown the inaccuracies of CFD models on the flow through a diffuser, creating a need for experimental data to back up model predictions. Experimental research however has focused primarily on two-dimensional studies of diffusers to reduce complexity of design and experimental procedure. This however has limited the validity of experimental data to real world turbine scenarios as the three dimensionality of the flow can change the problem very much. Additionally, the works that have studied three-dimensional diffusers were always lacking some critical component to lend the results more directly to a real world turbine environment; separation was not studied, or more so avoided, the three-dimensional diffuser was not of an annular design, and sometimes the Reynolds numbers were not very close to those found in the combustor-diffuser system of interest.

The work presented here has investigated a three-dimensional annular diffuser to characterize the flow, mainly that of the separation caused by a large diffusion angle. Where this flow characterization is a prerequisite for the advancement of an active separation control within the combustor-diffuser system of a gas turbine. The pressure recovery was measured on a naturally separated annular diffuser and compared with earlier works and a two-dimensional computational model. The data matched the trends of earlier works quite well, where the pressure recovery trend was typically the same for

different cases but with a larger total recovered pressure for a larger Reynolds number. Although it was unexpected to see the experimental data correlate with the CFD predictions, it was found that the model predicted very accurately the flow at the larger Reynolds number of 100,000.

The most important finding was the correlation between the dump gap and the amount of pressure recovery. Three dump gaps were tested, and it was found that the maximum pressure recovery existed at the smallest dump gap. This occurs as the dump wall gets close enough to the diffuser exit to cause the flow separation to switch from a jet-like separation leaving the wall to a separation bubble completely within the diffuser. However, there is a downside; the largest amount of flow distortion at the exit of the diffuser also existed with the smallest dump gap. This finding suggests that a careful design strategy must be used to choose the appropriate dump gap to gain desired pressure recovery yet resist too much outlet flow distortion. The use of an active separation control, such as the dielectric barrier discharge plasma actuator, could alleviate the need for the dump wall to aid in pressure recovery.

These results were also compared against another diffuser model whose geometries were consistent with the General Electric 8362 turbine CD diffuser. The comparison was able to show that for a diffuser with normally attached flow the pressure recover continues to increase throughout the diffuser, with a very steep pressure rise in the first 40 percent of the diffuser. The important point to get is that the separated diffuser experienced flow separation within the first 20 percent of the diffuser. Therefore, a large amount of the pressure recovery has been lost solely by the fact that the separation happened so early

on. Even if a plasma discharge could only delay separation there would still be huge benefits of such a device.

History tells us that in the turbine world we only see huge advancements when, as a society, we need them. Unfortunately, there is often a need for these advancements much before the knowledge exists to create them. For instance, the Romans could have very well benefited from the use of a water turbine, and they surely had the technology to machine and build such a machine. But instead they build water mills. Why? Because they lacked the knowledge of hydrodynamics and mechanics that was later acquired over many centuries. In the nineteenth century the same sort of problem began to exist. Energy demands stressed the need for gas turbines, but repeated attempts at making one was unsuccessful, mainly due to the lack of knowledge in fluid mechanics. However, the urgent need for the gas turbine incentivized many developments in related fields that in the end have been fruitful in gas turbine development. The lesson here is that the history of a technology is just as much about the development of that technology as it is the background and incentive for development. If we are to truly see great advancements in turbine technology, including low loss diffusers using separation control techniques, we must first establish the incentive for making such an advancement. I will leave it at that.

APPENDIX A: DOMINANCE OF TURBO-BASED POWER GENERATION

DOE – Annual Energy Outlook

	2008 (Billion kW-hr)	2030 (Billion kW-hr)
Turbo-Based	3725	4590
Non-Turbo-Based	120	150
PV Based	2	10
Electrochemical Based	0	0
Fuel Type	**2008 (Billion kW-hr)**	**2030 (Billion kW-hr)**
Geothermal	20	50
Solar	2	10
Wind	60	125
Biomass	50	150
MSW/LFG	15	15
Natural Gas	850	800
Coal	2000	2700
Nuclear	750	800
Petroleum	100	100

APPENDIX B: DRAWINGS

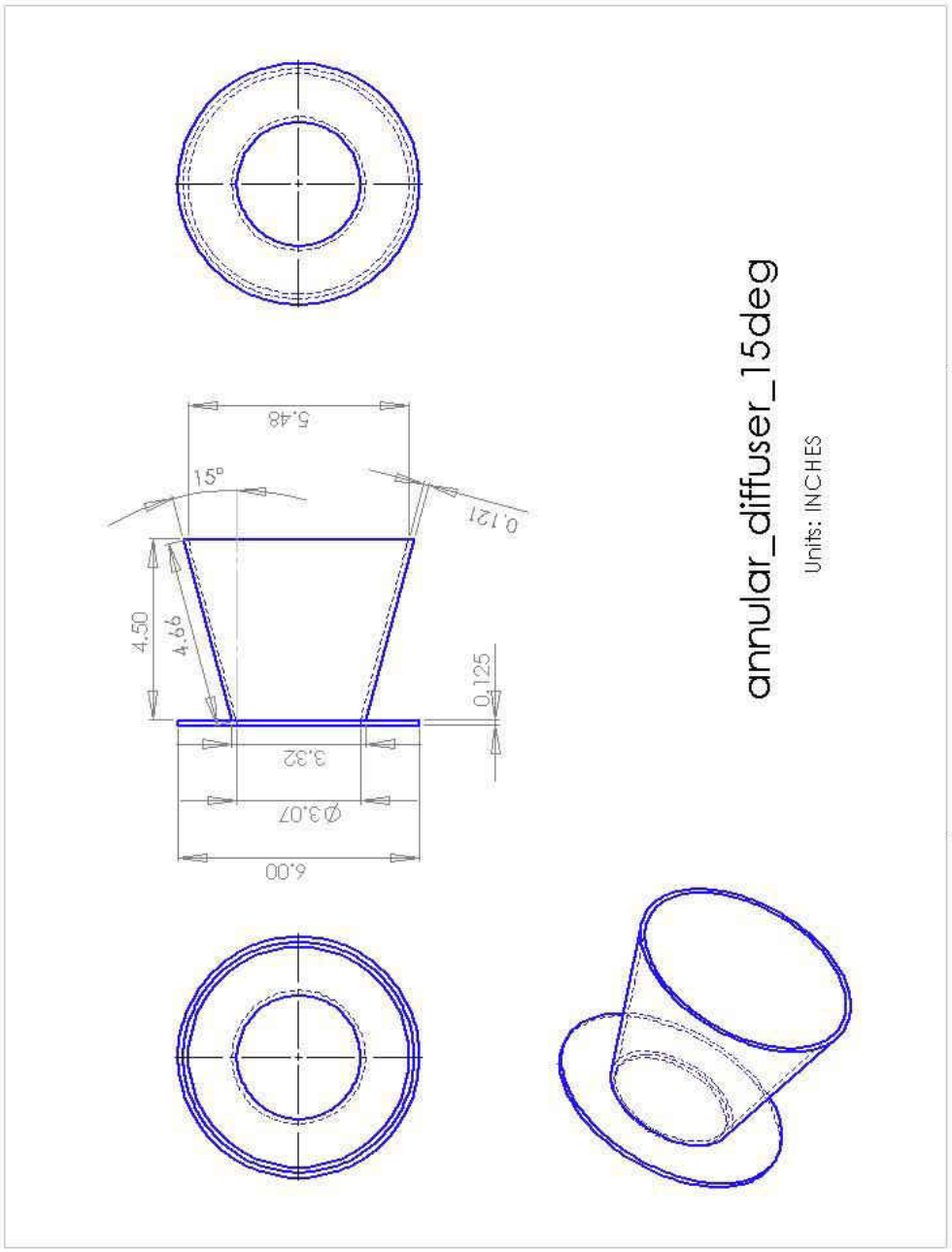

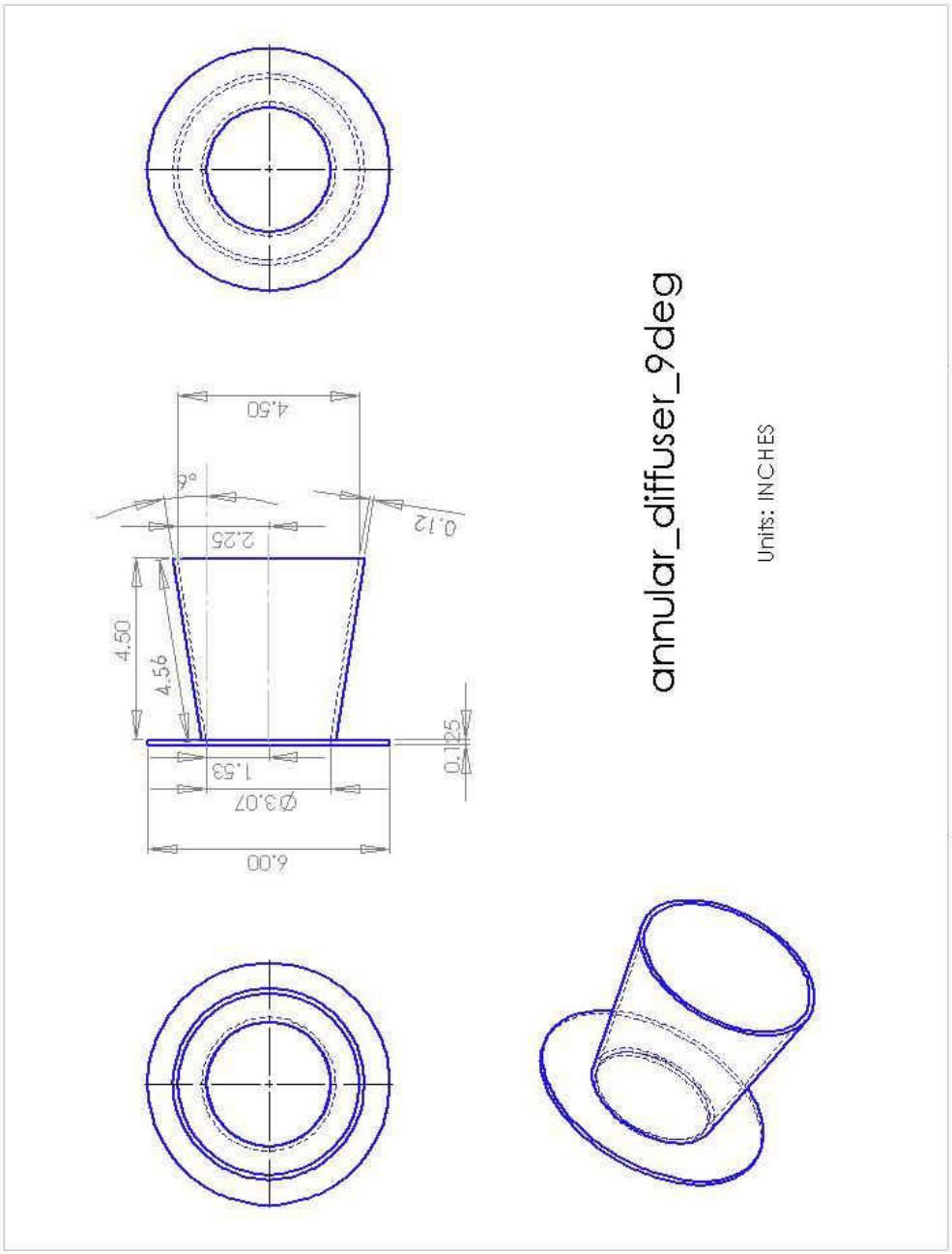

APPENDIX C: EXPERIMENTAL DATA

Pressure Variation Data on Diffuser 2

Re=100,000			Row 1	Row 2	Row 3
Tap #	**Location (cm)**	**x/L**	**Static Pressure (kPa)**	**Static Pressure (kPa)**	**Static Pressure (kPa)**
Pinlet	0	0	99.52597546	99.52597546	99.52597546
1	1.9304	0.16	99.96525594	99.84342758	99.91834261
2	2.4384	0.21	99.98933013	99.87870575	99.96025124
3	2.9464	0.25	99.97616115	99.94311427	99.98046437
4	3.4544	0.29	99.99636279	99.94265462	100.0097556
5	3.9624	0.33	99.99820139	99.97165857	99.99913768
6	4.4704	0.38	100.0068773	99.99083749	100.0170985
7	4.9784	0.42	100.0198165	100.0149232	100.0224534
8	5.4864	0.46	100.0253897	100.0304249	100.0266707
9	5.9944	0.51	100.0138065	100.0399511	100.0181787
10	6.5024	0.55	100.015174	100.0448349	100.0690045
11	7.0104	0.59	100.0325718	100.0515688	100.0415404
12	7.5184	0.64	100.0318133	100.0699778	100.0392077
13	8.0264	0.68	100.0234362	100.0784469	100.0458037
14	8.5344	0.72	100.0516472	100.092742	100.0563182
15	9.0424	0.76	100.0614608	100.0882144	100.0698089
16	9.5504	0.81	100.074354	100.0928454	100.0744744
17	10.0584	0.85	100.0896374	100.1198039	100.0758189
18	10.5664	0.89	100.0848225	100.1244234	100.088827
19	11.0744	0.94	100.1052655	100.1253427	100.0928259
20	11.5824	0.98	100.0960265	100.1289165	100.0772093

Row 4	Average	Percentage Error	
Static Pressure (kPa)	Static Pressure (kPa)		Cp
99.52597546	99.52597546	0.016480874	0
99.96406684	99.92277324	0.016415427	0.283212
99.98479708	99.95327105	0.016410419	0.304979
99.99287544	99.97315381	0.016407155	0.319171
99.99510474	99.98596944	0.016405052	0.328318
100.0185584	99.99688901	0.01640326	0.336111
99.99762133	100.0031087	0.01640224	0.340551
100.0200408	100.0193085	0.016399584	0.352113
100.0231434	100.0264072	0.01639842	0.35718
100.0222816	100.0235545	0.016398888	0.355144
100.0331178	100.0405328	0.016396104	0.367262
100.0383349	100.041004	0.016396027	0.367598
100.0508259	100.0479562	0.016394888	0.37256
100.0398058	100.0468731	0.016395065	0.371787
100.0547904	100.0638745	0.01639228	0.383922
100.0657645	100.0713122	0.016391061	0.38923
100.0750609	100.0791837	0.016389772	0.394849
100.065167	100.0876068	0.016388393	0.400861
100.0679938	100.0915167	0.016387753	0.403651
100.0710275	100.0986154	0.01638659	0.408718
100.1463872	100.1121349	0.016384378	0.418367

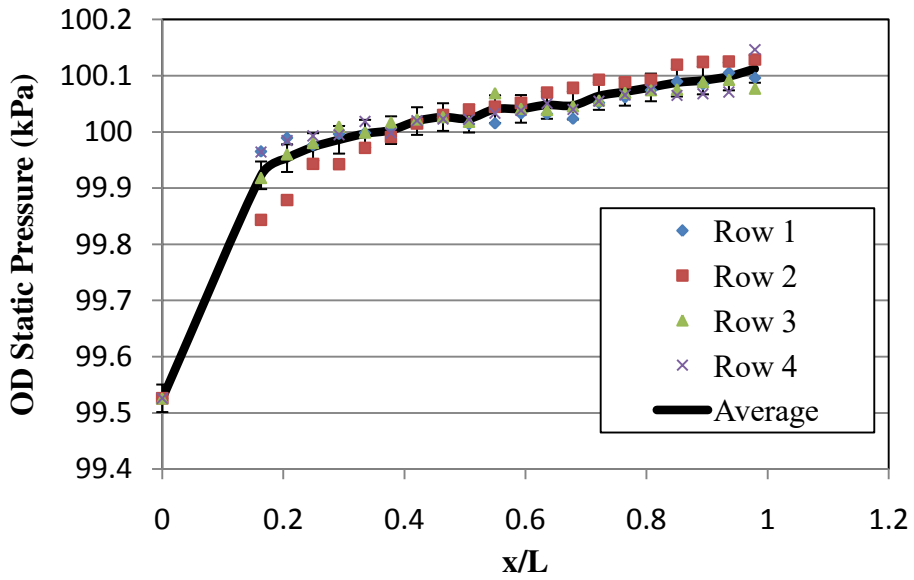

Diffuser 2 Static Pressure Recovery Data

Dump Gap Ratio = 0.5							
Re=50,000			Row 1		ID	cp	Cp
Tap #	Location (cm)	x/L	Static Pressure (kPa)	x/L	Static Pressure (kPa)	Re = 50,000	Re = 50,000
Pinlet	0	0	100.0036066	0	99.95597535	0	0
1	1.9304	0.16	100.0572134	0.2	100.0330013	0.204312829	0.14219295
2	2.4384	0.21	100.0641196	0.4	100.0807934	0.331082492	0.160511913
3	2.9464	0.25	100.0704053	0.6	100.0797822	0.328400181	0.177184913
4	3.4544	0.29	100.0671648	1	100.1950511	0.634153125	0.168589326
5	3.9624	0.33	100.0707271	1.2	100.2175854	0.693925982	0.178038376
6	4.4704	0.38	100.0754385				0.190535505
7	4.9784	0.42	100.0777138				0.196570704
8	5.4864	0.46	100.0784147				0.198430033
9	5.9944	0.51	100.0763004				0.192821566
10	6.5024	0.55	100.0792651				0.200685613
11	7.0104	0.59	100.0811841				0.205775907
12	7.5184	0.64	100.0799201				0.202423019
13	8.0264	0.68	100.0807819				0.204709079
14	8.5344	0.72	100.0876192				0.222845157
15	9.0424	0.76	100.0981338				0.250735093
16	9.5504	0.81	100.1011215				0.258660102
17	10.0584	0.85	100.1131988				0.290695427
18	10.5664	0.89	100.1308494				0.337513942
19	11.0744	0.94	100.1642085				0.425999715
20	11.5824	0.98	100.1852375				0.481779587

Re=100,000			OD		ID	Cp, DGR = 0.5, Re = 100,000	Cp
Tap #	**Location (cm)**	**x/L**	**Static Pressure (kPa)**	**x/L**	**Static Pressure (kPa)**	**Re = 100,000**	**Re = 100,000**
Pinlet	0	0	99.74582315	0	99.57063886	0	0
1	1.9304	0.16	99.93866951	0.2	99.9167212	0.23635864	0.131705372
2	2.4384	0.21	99.9683974	0.4	100.1037415	0.364085069	0.152008185
3	2.9464	0.25	99.99414932	0.6	100.0026758	0.295061785	0.169595584
4	3.4544	0.29	100.024153	1	100.5863056	0.693654572	0.190086749
5	3.9624	0.33	100.0182695	1.2	100.6155048	0.713596375	0.186068566
6	4.4704	0.38	100.0337942				0.196671233
7	4.9784	0.42	100.0334035				0.1964044
8	5.4864	0.46	100.041229				0.201748898
9	5.9944	0.51	100.0458025				0.204872407
10	6.5024	0.55	100.043263				0.203137996
11	7.0104	0.59	100.0523526				0.209345775
12	7.5184	0.64	100.0439065				0.203577485
13	8.0264	0.68	100.0746916				0.224602315
14	8.5344	0.72	100.0677738				0.21987781
15	9.0424	0.76	100.108338				0.2475813
16	9.5504	0.81	100.1544639				0.279083228
17	10.0584	0.85	100.2548056				0.347612087
18	10.5664	0.89	100.2771217				0.362852931
19	11.0744	0.94	100.4398264				0.473972962
20	11.5824	0.98	100.4767708				0.499204327

Dump Gap Ratio = 1

Re=50,000			Row 1		ID	Cp, DGR = 1, Re = 50,000	Cp
Tap #	Location (cm)	x/L	Static Pressure (kPa)	x/L	Static Pressure (kPa)	Re = 50,000	Re = 50,000
Pinlet	0	0	99.91851698	0	99.88551407	0	0
1	1.9304	0.16	99.96772256	0.2	99.94721066	0.163651436	0.130518802
2	2.4384	0.21	99.96473483	0.4	99.9892457	0.275150217	0.122593793
3	2.9464	0.25	99.97527232	0.6	99.99407203	0.287952155	0.150544691
4	3.4544	0.29	99.98337366	1	100.0431512	0.418135668	0.172033657
5	3.9624	0.33	99.98882052	1.2	100.099355	0.56721728	0.186481558
6	4.4704	0.38	99.99172781				0.194193202
7	4.9784	0.42	99.99947292				0.214737264
8	5.4864	0.46	100.0018976				0.221168713
9	5.9944	0.51	99.99913967				0.21385332
10	6.5024	0.55	100.0070916				0.234946037
11	7.0104	0.59	100.0116881				0.247138358
12	7.5184	0.64	100.008551				0.238817099
13	8.0264	0.68	100.0163191				0.259422122
14	8.5344	0.72	100.0203181				0.270029442
15	9.0424	0.76	100.0207432				0.271157232
16	9.5504	0.81	100.0260407				0.285208882
17	10.0584	0.85	100.0337054				0.305539578
18	10.5664	0.89	100.0332572				0.304350827
19	11.0744	0.94	100.0354865				0.310264103
20	11.5824	0.98	100.0357393				0.310934681

Re=100,000			OD		ID	Cp, DGR = 1, Re = 100,000	Cp
Tap #	Location (cm)	x/L	Static Pressure (kPa)	x/L	Static Pressure (kPa)	Re = 100,000	Re = 100,000
Pinlet	0	0	99.50992792	0	99.42667372	0	0
1	1.9304	0.16	99.66974839	0.2	99.62373738	0.134585593	0.10915018
2	2.4384	0.21	99.65944073	0.4	99.80824108	0.260593307	0.102110511
3	2.9464	0.25	99.70777298	0.6	99.7815239	0.242346675	0.135119258
4	3.4544	0.29	99.74294773	1	100.0771596	0.444252532	0.159142029
5	3.9624	0.33	99.78276495	1.2	100.1887627	0.520472445	0.186335398
6	4.4704	0.38	99.79984097				0.197997547
7	4.9784	0.42	99.83316563				0.220756788
8	5.4864	0.46	99.84734585				0.230441237
9	5.9944	0.51	99.86811056				0.244622599
10	6.5024	0.55	99.88500271				0.256159179
11	7.0104	0.59	99.89331089				0.261833293
12	7.5184	0.64	99.91065121				0.273675947
13	8.0264	0.68	99.93310514				0.289010966
14	8.5344	0.72	99.93112864				0.287661108
15	9.0424	0.76	99.94822764				0.299338953
16	9.5504	0.81	99.97249718				0.315913958
17	10.0584	0.85	99.97341648				0.3165418
18	10.5664	0.89	99.98771161				0.326304729
19	11.0744	0.94	100.0077983				0.340023058
20	11.5824	0.98	100.001053				0.335416273

Dump Gap Ratio = Inf							
Re=50,000			Row 1		ID	Cp, DGR = ∞, Re = 50,000	Cp, DGR = ∞, Re = 50,000
Tap #	Location (cm)	x/L	Static Pressure (kPa)	x/L	Static Pressure (kPa)	Re = 50,000	Re = 50,000
Pinlet	0	0	99.92176901	0	99.90042973	0	0
1	1.9304	0.16	99.95742639	0.2	99.94695785	0.123416775	0.094581935
2	2.4384	0.21	99.96095421	0.4	99.99372729	0.247473647	0.103939541
3	2.9464	0.25	99.96894064	0.6	99.99377325	0.24759557	0.1251237
4	3.4544	0.29	99.98314384	1	100.0372102	0.362813009	0.162797974
5	3.9624	0.33	99.98817701	1.2	100.0378422	0.364489453	0.176148566
6	4.4704	0.38	100.0011966				0.210683317
7	4.9784	0.42	99.99971424				0.206751293
8	5.4864	0.46	100.0048738				0.220437174
9	5.9944	0.51	100.0096887				0.233208631
10	6.5024	0.55	100.0168132				0.252106729
11	7.0104	0.59	100.0200308				0.260641354
12	7.5184	0.64	100.0225474				0.26731665
13	8.0264	0.68	100.0279483				0.281642628
14	8.5344	0.72	100.0299937				0.287068211
15	9.0424	0.76	100.0291089				0.284721189
16	9.5504	0.81	100.033602				0.296639184
17	10.0584	0.85	100.0301086				0.287373019
18	10.5664	0.89	100.0347511				0.299687264
19	11.0744	0.94	100.0369804				0.30560054
20	11.5824	0.98	100.0314531				0.290939273

Re=100,000			OD		ID	Cp, DGR = ∞, Re = 100,000	Cp, DGR = ∞, Re = 100,000
Tap #	Location (cm)	x/L	Static Pressure (kPa)	x/L	Static Pressure (kPa)	Re = 100,000	Diffuser 2 Re = 100,000
Pinlet	0	0	99.52597546	0	99.52414835	0	0
1	1.9304	0.16	99.60757492	0.2	99.62823621	0.071087311	0.055728748
2	2.4384	0.21	99.66307771	0.4	99.80598305	0.192480393	0.093634656
3	2.9464	0.25	99.70372231	0.6	99.82752916	0.207195419	0.121393082
4	3.4544	0.29	99.75704176	1	99.97196284	0.305837108	0.157807867
5	3.9624	0.33	99.78757405	1.2	100.0119524	0.333148197	0.17866004
6	4.4704	0.38	99.81822124				0.199590694
7	4.9784	0.42	99.84566238				0.218331751
8	5.4864	0.46	99.861934				0.229444539
9	5.9944	0.51	99.87385044				0.23758293
10	6.5024	0.55	99.90167079				0.256582972
11	7.0104	0.59	99.91216231				0.263748209
12	7.5184	0.64	99.92650341				0.27354253
13	8.0264	0.68	99.94376328				0.285330248
14	8.5344	0.72	99.9555763				0.293398006
15	9.0424	0.76	99.96206886				0.297832134
16	9.5504	0.81	99.97535276				0.306904438
17	10.0584	0.85	99.98777482				0.315388141
18	10.5664	0.89	99.98243138				0.311738815
19	11.0744	0.94	100.0109872				0.33124113
20	11.5824	0.98	100.0063447				0.328070532

Diffuser 1 Pressure Recovery Data

Re=50,000			Average	Cp	Re=100,000			Average	Cp
Tap #	**Location (cm)**	**x/L**	**Static Pressure (kPa)**	**Re = 50,000**	**Tap #**	**Location (cm)**	**x/L**	**Static Pressure (kPa)**	**Re = 100,000**
Pinlet	0	0	99.77	0	Pinlet	0	0	99.05	0
1	1.9304	0.16	99.91038116	0.400784437	1	1.9304	0.16	99.49650421	0.362871318
2	2.4384	0.21	99.93011166	0.457114473	2	2.4384	0.21	99.56003939	0.414505989
3	2.9464	0.25	99.94970426	0.513050823	3	2.9464	0.25	99.62778039	0.469558689
4	3.4544	0.29	99.95972464	0.541658739	4	3.4544	0.29	99.68836232	0.518793268
5	3.9624	0.33	99.97483565	0.584800264	5	3.9624	0.33	99.740073	0.56081823
6	4.4704	0.38	99.99216448	0.633773587	6	4.4704	0.38	99.80664188	0.614418365
7	4.9784	0.42	99.99294588	0.63650448	7	4.9784	0.42	99.8106868	0.618205651
8	5.4864	0.46	100.000714	0.658682176	8	5.4864	0.46	99.84088584	0.642748229
9	5.9944	0.51	100.0043337	0.669016458	9	5.9944	0.51	99.87643981	0.671642726
10	6.5024	0.55	100.0129866	0.693720312	10	6.5024	0.55	99.89403293	0.685940552
11	7.0104	0.59	100.0174797	0.706547944	11	7.0104	0.59	99.9093278	0.698370602
12	7.5184	0.64	100.0205479	0.715307478	12	7.5184	0.64	99.92479504	0.710940735
13	8.0264	0.68	100.0274312	0.734959017	13	8.0264	0.68	99.94380159	0.726387243
14	8.5344	0.72	100.0279598	0.73646815	14	8.5344	0.72	99.96248638	0.741572263
15	9.0424	0.76	100.0337284	0.752937386	15	9.0424	0.76	99.97622993	0.752741564
16	9.5504	0.81	100.033602	0.752576506	16	9.5504	0.81	99.98935295	0.763406566
17	10.0584	0.85	100.0368195	0.761762535	17	10.0584	0.85	99.99669587	0.769374111
18	10.5664	0.89	100.0363139	0.760319016	18	10.5664	0.89	100.0056016	0.776611743
19	11.0744	0.94	100.0412437	0.774393323	19	11.0744	0.94	100.016208	0.78523153
20	11.5824	0.98	100.0428984	0.779117566	20	11.5824	0.98	100.0291932	0.795784465

APPENDIX D: NUMERICAL PRESSURE RECOVERY CALCULATIONS

Estimated Pressure Recovery on Diffuser 1 | Re = 50,000

$A_R := 2.($ $\quad v_1 := 24.759\frac{m}{s}$ $\quad \rho := 1.23\frac{kg}{m^3}$ $\quad q_1 := 0.5\rho \cdot v_1^{\,2}$ $\quad v_2 := \frac{v_1}{A_R}$

$P_1 := 99.771 10^3 Pa$ $\quad P_2 := 100.051 10^3 Pa$ $\quad P_{01} := P_1 + 0.5\rho \cdot v_1^{\,2}$ $\quad P_{02} := P_2 + 0.5\rho \cdot v_2^{\,2}$

Find Ideal Pressure Recovery Coefficient

$$C_{pi} := 1 - \frac{1}{A_R^{\,2}} \qquad C_{pi} = 0.852$$

Find Actual Pressure Recovery Coefficient

$$C_p := C_{pi} - \frac{P_{01} - P_{02}}{q_1} \qquad C_p = 0.743$$

Diffuser Effectiveness

$$\eta_D := \frac{C_p}{C_{pi}} \qquad \eta_D = 0.872$$

Note: The value for the static pressure at the inlet is based off the measured value during the test, and value for the static pressure at the exit is equal to the ambient pressure, since the flow is subsonic.

Estimated Pressure Recovery on Diffuser 1 | Re = 100,000

$A_R := 2.($ $\quad v_1 := 48.794\frac{m}{s}$ $\quad \rho := 1.23\frac{kg}{m^3}$ $\quad q_1 := 0.5\rho \cdot v_1^{\,2}$ $\quad v_2 := \frac{v_1}{A_R}$

$P_1 := 99.0510^3 Pa$ $\quad P_2 := 100.0510^3 Pa$ $\quad P_{01} := P_1 + 0.5\rho \cdot v_1^{\,2}$ $\quad P_{02} := P_2 + 0.5\rho \cdot v_2^{\,2}$

Find Ideal Pressure Recovery Coefficient

$$C_{pi} := 1 - \frac{1}{A_R^{\,2}} \qquad C_{pi} = 0.852$$

Find Actual Pressure Recovery Coefficient

$$C_p := C_{pi} - \frac{P_{01} - P_{02}}{q_1} \qquad C_p = 0.683$$

Diffuser Effectiveness

$$\eta_D := \frac{C_p}{C_{pi}} \qquad \eta_D = 0.802$$

Note: The value for the static pressure at the inlet is based off the measured value during the test, and value for the static pressure at the exit is equal to the ambient pressure, since the flow is subsonic.

LIST OF REFERENCES

Adenubi, S. O. 1975. "Performance and flow regime of annular diffusers with axial turbomachine-discharge inlet conditions." Paper 75-WA/FE 5. ASME, New York.

Agrawal, A. K., Kapat, J. S., Yang, T. T., 1998 "An experimental/computational study of airflow in the combustor-diffuser system of a gas turbine for power generation." Transactions of the ASME, Vol. 120, pp. 24-33.

Cherry, E.M., Elkins, C.J., Eaton, J.K., 2008, "Geometric sensitivity of three-dimensional separated flows." International Journal of Heat and Fluid Flow, Vol. 29, pp. 803-811.

Cherry, E.M., Elkins, C.J., Eaton, J.K., 2009, Letters to the Editors "Pressure measurements in a three-dimensional separated diffuser." International Journal of Heat and Fluid Flow, Vol. 30, pp. 1-2.

Corke, Thomas C., Post M. L., Orlov D. M., 2009 "Single dielectric barrier discharge plasma enhanced aerodynamics: physics, modeling and applications." Exp Fluids, Vol. 46, pp. 1-26.

Dixon, S.L. 2005, *Fluid Mechanics and Thermodynamics of Turbomachinery.* Elsevier Butterworth-Heinemann, Burlington, MA. pp.44-49.

Fishenden, C. R., Stevens S. J., 1977. "Performance of annular combustor-dump diffusers." Journal of Aircraft, Vol. 14, pp.60-67.

Jayaraman, B., Cho Y., Shyy W., 2008. "Modeling of dielectric barrier discharge plasma actuator." Journal of Applied Phyiscs. Vol. 103, 053304.

Kaltenbach, H. J., Fatica, H., Mittal, R., Lund, T.S., Moin, 1999. "Study of flow in a planar asymmetric diffuser using large-eddy simulation." Journal of Fluid Mechanics., Vol. 390, pp. 151-185.

Klein, A., 1995, "Characteristics of Combustor Diffusers." *Proceedings of the Aerospace Science*, Vol. 31, pp. 171-271.

Kline, S. J., McClintock, F.A., 1953, "Describing Uncertainties in single-Sample Experiments." Mechanical Engineering, 75, pp. 3-7.

Likhanskii, A. V., Shneider, M. N., Macheret, S. O., Miles, R. B., 2008. "Modeling of dielectric barrier discharge plasma actuator in air." Journal of Applied Physics. Vol. 103, 053305.

Mellen, C.P., Frohlich, J., Rodi, W., 2003. "Lessons from LESFOIL project on large-eddy simulation of flow around an airfoil." AIAA Journal, Vol. 41 (4), pp. 573-581.

Obi, S., Aoki, K., Masuda, S., 1993. "Experimental and computational study of separating flow in an asymmetric plane diffuser." 9th Symposium on Turbulent Shear Flows, Kyoto, Japan, August 16-18, 1993.

Quirke, Brian. Follow the Green Money Tour. 17 August 2009.

Reneau, L. R., Johnston, J. P., & Kline, S. J. (1964) *Performance and Design of Straight Two-Dimensional Diffusers*. Report PD-8, Thermosciences Division, Mechanical Engineering Department, Stanford University, September 1964.

Singh, K. P., Roy, S., 2008. "Force approximation for a plasma actuator operating in atmospheric air." Journal of Applied Physics, Vol. 103, 013305.

Sovran, G., Klomp, E.D., 1967,. "Experimentally determined optimum geometries for rectilinear diffusers with rectangular, conical, or annular cross sections." In: Sovran, Gino (Ed.), *Fluid Mechanics of Internal Flow*, Elsevier Publishing Company, New York, pp. 272-319.

Srinivasan, R., Freeman, W. G., Grahmann, J., Coleman, E., 1990. "Parametric Evaluation of the Aerodynamic Performance of an Annular Combustor-Diffuser System." AIAA Paper No. 90-2163.

Wilson, D. G. 1984, *The Design of High-Efficiency Turbomachinery and Gas Turbines.* The MIT Press, Cambridge, MA. pp.147-187.